Title

USE OF EXCESS CARBON-14 DATA TO CALIBRATE MODELS OF STRATOSPHERIC OZONE DEPLETION BY SUPERSONIC TRANSPORTS

Authors

Johnston, Harold S.
Kattenhorn, David
Whitten, Gary.

Publication Date

1975-06-01

Submitted to Journal of Geophysical Research

LBL-3548 Rev.
Preprint

USE OF EXCESS CARBON-14 DATA TO CALIBRATE MODELS OF STRATOSPHERIC OZONE DEPLETION BY SUPERSONIC TRANSPORTS

Harold S. Johnston, David Kattenhorn,
and Gary Whitten

June 1975

Prepared for the U.S. Energy Research and
Development Administration under Contract W-7405-ENG-48

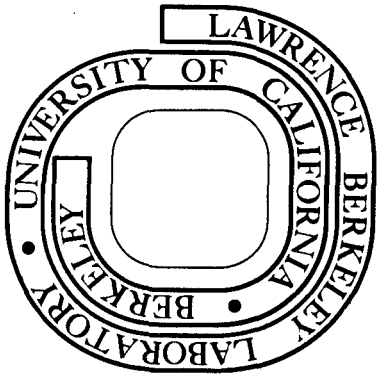

DISCLAIMER

USE OF EXCESS CARBON-14 DATA TO CALIBRATE MODELS OF STRATOSPHERIC OZONE DEPLETION BY SUPERSONIC TRANSPORTS

Harold S. Johnston
Department of Chemistry
University of California
and
David Kattenhorn
Gary Whitten
Inorganic Materials Research Division
Lawrence Berkeley Laboratory
Berkeley, California

ABSTRACT

During 1974, at least seven one-dimensional models of vertical eddy transport and photochemistry have been used to predict the reduction of ozone by nitrogen oxides from supersonic transports. Chang (1974) has shown that these predictions are sensitive to the assumed values for the vertical eddy diffusion coefficient K_z. In this article, an effort is made to calibrate the one-dimensional K_z functions against quantitative data for the dissipation of excess carbon-14 from the stratosphere during the period 1963-70. The data for excess carbon-14, following the nuclear bomb test series of 1961-62, were published in 1971 and 1972, and these data were not used to derive the various K_z functions. Tables of data are presented in a form that may be useful to others in calibrating two-dimensional and three-dimensional models of stratospheric motion. In checking the one-dimensional models, the direct observations by balloons at 30°N are primarily used. Also, these data are interpreted as a special hemispherical average (averaging along lines parallel to a standard, sloping tropopause). The carbon-14 data and strontium-90 data differ in many important respects, and it is judged that the carbon-14 data give the better estimate of air motion in the stratosphere. The seven K_z models give predictions that strongly differ from one model to another. The models that give a fairly realistic prediction of carbon-14 distribution and persistence are those with minimum K_z between 15 and 20 km and with increasing K_z from 20 to 50 km. Models with these features, as recalculated by Chang (1974), agree with each other as to ozone reduction by artificial nitrogen oxides from SSTs. These models are used to predict the ozone reduction by SSTs according to Grobecker's (1974) upper-bound projection out to the year 2025. Very large reductions of global ozone are indicated - more than a factor of two.

INTRODUCTION

The catalytic reduction of stratospheric ozone by nitrogen oxides from supersonic transport (SST) exhausts was calculated by means of a "box model" and steady-state photochemistry (Johnston, 1971). At that time, the natural background of nitrogen oxides (NO_x) was not known, the quantity of NO_x expected to be emitted by future SST fleets was uncertain, and the photochemical-atmospheric model was primitive, though efficient. By the end of 1974, these uncertainties have been greatly reduced. During 1974, a substantial number of measurements of NO_x in the stratosphere have been reported and are summarized by Hard (1974). Grobecker (1974) has published a projection for the years 1990-2025 of future SST traffic in the stratosphere, and he gave an estimate of the amount of nitrogen oxides that would be emitted in the stratosphere at various altitude bands if future SSTs emit NO_x at the same rate as present ones. Model calculations of the natural stratosphere and the stratosphere as perturbed by SSTs have been made by at least seven different one-dimensional modelers including vertical eddy transport and extensive O, N, H chemistry (Crutzen, 1974; Chang, 1974; Stewart, 1973; McElroy et al, 1974; Whitten and Turco, 1974; Shimazaki and Ogawa, 1974; Hunten, 1974). Similar calculations have been made including two-dimensional motions by at least three groups (Hesstvedt, 1974; Vupputuri, 1974; and Widhopf, 1974). One group has successfully carried out calculations of the SST perturbation problem with a model of three-dimensional atmospheric motions (Cunnold et al, 1974). Model calculations of ozone reduction by injection of NO_x at 20 km are given by Figure 1, panel A.

To a considerable extent, these twelve calculations of the SST perturbation (1971-1974) are in agreement; ten out of twelve agree better than a factor of three; but two of them fall far outside this range. Chang (1974) undertook a systematic investigation of the reasons for the discrepancies between the one-dimensional models. He found that Stewart (model 5) had carried out integrations of the SST perturbation for only 18 months, whereas at least 10 years are needed to attain a steady state; this correction brought model 5 into line with ten others. Chang (1974) used his chemical model, his set of boundary conditions, and his computer program to recalculate the predicted SST effect for the seven models involving one-dimensional motions, Figure 1, panel B. The seven vertical eddy diffusion functions, K_z, are given in Figure 2 and in Appendix Table A1. The maximum rate of insertion of nitrogen oxides in Figure 1B corresponds to Grobecker's (1974) upper bound projection for the year 2025.

The curves in Figure 1B differ only with respect to vertical eddy diffusion function, K_z. At low values of NO_x injection rate, there is a spread of a factor of 6 between model 7 and model 12; and at high rates of NO_x injection this spread is a factor of 3. The purpose of this paper is to see if an independent evaluation can be made to assess the accuracy of the seven K_z functions, and to narrow the spread of predictions in Figure 1B.

During and after the period of massive nuclear bomb tests of 1961-62, there was extensive sampling of the stratosphere for radioactive

tracers, including those lodged on solid particles such as strontium-90 and those as gases such as excess carbon-14. There are detailed, zonal-average, contour maps of observed excess carbon-14 in the stratosphere and troposphere every three months (with a few exceptions) from 1955 to 1967 (Telegadas, 1971) and some further data out to 1971 (Telegadas et al, 1972). These data were only recently published in the form of Health and Safety Laboratory (HASL) Reports of the U.S. Atomic Energy Commission. (We obtained HASL reports as microfilm copies in the Documents Library of the University of California, Berkeley). It appears that none of the modellers of the SST perturbation made detailed, quantitative use of these extensive data. After the end of the test series in December 1962, there was a cloud of carbon-14 covering the northern hemisphere with peak concentration at about 19 or 20 kilometers and with a fairly narrow vertical spread. This case is an appropriate analogy for the SST problem.

In this article, we develop the data in a form that may be useful for testing two and three dimensional models of stratospheric motion, and tables are given in the appendix for this purpose. We take the data at 30°N as primary source for testing the one-dimensional models. However, we carry out an averaging process over the northern hemisphere, to supplement the direct observations at 30°N and, perhaps, to interpret what a one-dimensional model does. We then take an observed distribution of excess carbon-14 as the initial condition; and we solve the time-dependent, one-dimensional, vertical eddy diffusion equations for subsequent distributions of excess carbon-14, using each of nine K_z functions (the seven used for the SST problem and two more). Numerous

initial and final states were treated. The merit of a given K_z function is judged with respect to how well it predicts the magnitude and shape of the carbon-14 profile as a function of time.

PRIMARY DATA

An example of the observed distribution of excess carbon-14 from the HASL Reports of the U.S. Atomic Energy Commission is shown in Figure 3 (Telegadas, 1971). The units are 10^5 atoms of excess carbon-14 per gram of air and are proportional to mixing ratio or mole fraction. By multiplying by 4.82×10^{-18}, one can convert these units to mixing ratio by volume. The data are from balloons, U-2 aircraft, and ordinary aircraft. Balloons were launched at 30°N for the period 1963-70 (after 1970 balloons were launched at latitudes of 65°N, 30°N, 9°N, and 34°S), and the observed excess carbon-14 is gives as numbers on Figure 3. Extensive sampling was done by U-2 aircraft in the stratosphere and by ordinary aircraft in the troposphere, and carbon-14 was measured at numerous ground-level stations.

It is important to emphasize that the numerical data points written in on Figure 3 are all the carbon-14 data observed for this time period (except for ground-based measurements). The only observations above 22 km are the balloon soundings at 30°N. It might appear that the contour lines above 22 km are largely the product of imagination on the part of the authors of the report, but such an appearance is not quite correct. More extensive data were obtained by balloon for other radioactive species, and these data were some guide to where bomb debris did and did not go. Data were obtained every 3 months before and after this period, and

continuity between one period and another was of some guidance in drawing the contour lines. Also the total stratospheric burden of carbon-14 was known. The bombs of high total yield (above 10 MT) had a smaller fraction of fission yield relative to total yield than smaller bombs. One bomb with about 60 MT total yield was fired at 75°N in October 1961, and it may constitute a hidden reservoir of carbon-14 above 35 or 40 km. The subsequent analysis of data depends primarily on the direct observations at 30°N, and these data are supplemented by a hemispherical average that is significant only below 22 km.

The balloon measurements of ^{14}C at 30°N (actually 31°N) for the period January 1963 to January 1966 (Telegadas, 1971) and for November 1970 (Telegadas et al, 1972) are listed in the Appendix, Table A2. From a series of contour maps similar to Figure 3, the mixing ratios were converted to concentration of excess carbon-14 by use of air density data from the Table of Standard Atmospheres. Vertical profiles were drawn at each 10 degrees of latitude, and these profiles were read at each kilometer elevation to give the values in the Appendix, Table A3. This analysis was carried out for January 1963, April 1963, July 1963, October 1963, January 1964, and January 1965. These data were replotted as zonal-average contour maps of excess carbon-14 concentration, five of which are given in Figure 4.

An example of the observed distribution of strontium-90 for April 1963 is shown in Figure 5 (Telegadas, 1967). The units are disintegrations per minute per thousand cubic feet of standard air and are proportional to mixing ratio. The elevations for various values of

strontium-90 mixing ratios at 30°N are given in the Appendix, Table A4. From these data, profiles of strontium-90 mixing ratios are readily obtained.

COMPARISON OF CARBON-14 AND STRONTIUM-90 AS TRACERS FOR STRATOSPHERIC AIR MOTIONS

Johnston, Whitten, and Birks (1973) showed that the bulk "residence time" of carbon-14 in the stratosphere (1963-65) was twice as long as that for strontium-90. There must be factors that cause strontium-90 to have a spuriously short residence time, or that cause carbon-14 to have (or appear to have) a spuriously long residence time, or both.

Carbon-14 is formed by a nuclear reaction between a neutron and molecular nitrogen. The initial product is probably ^{14}CO, not $^{14}CO_2$. The nuclear bombs of the 1961-62 test series were fired on the surface or in the troposphere, and the fireball was lifted into the stratosphere by thermal buoyancy. Before rising, the fireball cooled to about 6000°K by emission of radiation and by expansion. The rising fireball was further cooled largely by entrainment of cold air. The gases transported into the stratosphere were subjected to a wide range of temperatures from 6000°K to ambient. Carbon monoxide is burned to carbon dioxide by hot air. Measurements by Hagemann et al (1965) showed that much less than 1 percent of the carbon-14 was in the form of carbon monoxide and at least 99 percent was carbon-14 dioxide.

Strontium-90 was lodged on solid particles. One immediately suspects that the difference in stratospheric residence times between carbon-14 and strontium-90 is that particulate strontium-90 underwent gravitational

settling. However, Telegadas and List (1969) calculated the settling velocity of strontium-90 on the basis of estimates and some measurements of the size of the solid particles containing the radioactive tracer; they concluded that the settling velocity would be slow below 30 km. Their calculations did not consider the possibility that the radioactive particles would ionize the surrounding air and act as condensation nuclei for aqueous sulfuric acid in the stratosphere. Such enlarged particles would settle faster than the "dry" particles considered by Telegadas and List.

The carbon-14 and strontium-90 clouds at 30°N are directly compared with each other in Figure 6, using the data in Tables A2 and A4, and A6. For strontium-90, the maximum mixing ratio in April 1963 was 1700 units of Table A4. All strontium-90 mixing ratios for April 1963 and later times were divided by 1700 to normalize all observations to the maximum as of April 1963. For carbon-14 the maximum mixing ratio in April 1963 was 74.2 units of Table A.6, and all carbon-14 mixing ratios were normalized by this value. The curves in Figure 6 are the normalized strontium-90 mixing ratios for April 1963, January 1964, January 1965, and January 1966. The circles in Figure 6 are normalized, average carbon-14 mixing ratios (Table A6); and the triangles are normalized, directly observed carbon-14 mixing ratios (Table A2) for the same times as the strontium-90 curves.

In April 1963 the relative carbon-14 and strontium-90 profiles are very nearly the same above 14 km (Strontium-90 is washed out by rain in the troposphere, carbon-14 is not, and the differences between C-14 and Sr-90 in the troposphere is due to this feature). The agreement in

relative mixing ratios is good both above and below the point of maximum mixing ratios - for the April 1963 data. However, above 30 km strontium-90 is less than carbon-14. In January 1964 the carbon-14 and strontium-90 clouds agree fairly well below the maximum (15 to 20 km), but the relative mixing ratio of strontium-90 is substantially less than that of carbon-14 in the range 23 to 30 km. By January 1965, the strontium-90 is less than the carbon-14 over the range 18 to 30 km, and they are together 15 to 18 km. By January 1966, the relative mixing ratio of strontium-90 is at least a factor of two less than that of carbon-14 at all elevations.

The separation of the strontium-90 and carbon-14 clouds in Figure 6 appears to be due to gravitational settling. However, Chang (1975) offers an alternate explanation. Most of the tests of the 1961-62 series were at the polar USSR station, Table 1. The bomb debris deposited in the polar stratosphere would require time to appear at 30°N. The largest test was a 60 MT bomb, October 1961, which had an unusually small fission yield (strontium-90) but normal carbon-14 yield. This large bomb probably rose high in the stratosphere. As this debris was transported downwards, its high $^{14}C/^{90}Sr$ ratio would cause an apparent separation of the carbon-14 and strontium-90 clouds. This explanation concerns a region of the stratosphere where no observations were made. We believe that the difference between the C-14 and Sr-90 profiles in Figure 6 is too great to be explained quantitatively by this mechanism.

If the separation of clouds in Figure 6 is due to particulate settling by the strontium-90, then the carbon-14 data would be superior to the strontium-90 data (and probably to other solid, particulate, radioactive tracers) for the purpose of calibrating models of stratospheric motion.

TABLE 1

APPROXIMATE TIMES AND YIELDS (MT) OF NUCLEAR BOMB TESTS IN 1961-62;

MONTHS FROM BOMB EXPLOSION TO VARIOUS LATER TIMES.

Time mo/yr	Location*	MT	months from test until: 1/63	1/64	1/65
9/61	P	9.2	16	28	40
10/61	P	90.5	15	27	39
5/62	T	2	8	20	32
6/62	T	10	7	19	31
7/62	T	2	6	18	30
8/62	P	54	5	17	29
9/62	P	96	4	16	28
10/62	P,T	17	3	15	27
12/62	P	23	1	13	25
	Total:	304			
	Weighted average age of debris (mo.)		8	20	32

*P, polar, USSR; T, tropical, US or UK. (Seitz et al, 1968)

ANALYSIS OF THE CARBON-14 DATA

These data are based on a fairly thin grid so far as global coverage is concerned. There was detailed sampling by aircraft up to 22 km, but there was only one balloon profile of carbon-14 at higher elevation until 1970, compare Figure 3. There were more extensive balloon samples of strontium-90 than carbon-14, especially in the polar region (Telegadas, 1967). Seitz et al (1968) tabulated each explosion of the 1961-62 series (their tables 2-4) with respect to date, yield, and vertical distribution. Seitz et al pointed out that the observed distributions after the polar tests were quite different from those calculated on the basis of previous experience (1954-58) for tropical tests. If we assume a uniform distribution of nuclear bomb materials over their quoted vertical spread, then only 35 MT out of 304 MT of the large bombs was deposited above 22 km, that is, about 88 percent of the nuclear cloud was deposited in the region that was densely searched by aircraft. According to the tables by Seitz et al, the portion of nuclear debris above 33 km (the upper limit of the balloon measurements) was 4 MT out of 304 MT. If Seitz et al are correct, the amount of excess carbon-14 completely outside the range of observations was not large; but the two dimensional distribution of material between 22 and 33 km, is not accurately known.

There is a large error of measurement associated with any one contour map of carbon-14, and no conclusions should be based on minor features. There was a slow transport of carbon-14 from the northern hemisphere to

the southern hemisphere, as seen in Table 2. This movement of carbon-14 from the northern hemisphere to the southern hemisphere can be treated by a two or a three dimensional model of atmospheric motions. To a one-dimensional model, however, this loss to the southern hemisphere may appear as a faster than real loss to vertical transport.

It was suggested by Seitz et al (1968) that nuclear bomb debris be averaged over the northern hemisphere, not at equal heights above the ground but at equal heights above a sloping tropopause. The sloping lines of constant mixing ratio of carbon-14 are evident in Figure 3, and these lines more or less parallel the tropopause. Of course, there is a time-and-place varying gap in the tropopause. On a year-long basis it is possible to define and use the concept of a "standard tropopause", which we take to be:

90°N, 8 km	40°N, 13 km
80°N, 9 km	30°N, 14 km
70°N, 10 km	20°N, 15 km
60°N, 11 km	10°N, 16 km
50°N, 12 km	0°, 16 km

The observed concentrations in Table A3 of the Appendix were averaged by the cosine function to give equal weight to equal area over the three-dimensional globe along lines at equal heights above this "standard tropopause". This average over the northern hemisphere was assigned to 30°N latitude, the latitude of mid-area between the equator and the pole.

This choice of tropopause height is based on the observed slope with latitude of the maximum carbon-14 mixing ratio for a large number of maps,

TABLE 2

DISTRIBUTION OF CARBON-14 BETWEEN THE NORTHERN HEMISPHERE AND THE SOUTHERN HEMISPHERE FROM JANUARY 1963 TO DECEMBER 1970.

Date	Carbon-14 inventory in stratosphere in units of 10^{26} atoms			
	N.H.	S.H.	% N.H.	Ref.
1/63	310	(46)	87	a.
7/63	243	(58)	81	
1/64	203	(52)	80	
7/64	128	(55)	70	
1/65	113	(57)	66	
7/65	92	(59)	61	
1/66	88	(58)	61	
7/66	73	(55)	57	
7/69	45	(41)	52	

a. Telegadas, 1971

such as Figure 3, during the test moratorium of 1959-1961, and during the period 1963-67 (Telegadas, 1971). Within the somewhat coarse grid of the observations and within a fairly substantial noise factor in the data, the simple linear function (given above) for the average slope of lines of constant mixing ratio seemed as good as any other. It would be desirable to derive an appropriate slope from independent meteorological considerations, but such a study is beyond the scope of this article. Most conclusions of this article are based on actual observations by balloons at 30°N, not the hemisphere averages deduced in this way.

The average profiles ascribed to 30°N are listed in Table A5 of the appendix, and they are plotted in Figure 7, for the periods of January 1963, April 1963, July 1963, October 1963, January 1964, and January 1965. There are insufficient data to support this detailed analysis after 1965. These average-concentrations are converted to average-mixing-ratios at 30°N by dividing by total air concentration. These mixing ratios are listed in Table A6 of the appendix.

The hemisphere-average mixing-ratio profiles (Table A6) are plotted as circles in Figure 8 and the 30°N local profiles (Table A2) are plotted as triangles on the same figure. Comparisons between these two profiles are interesting only below 22 km, where aircraft carried out measurements at different latitudes (above 22 km, all data are based on balloons operated at only one latitude with interpolation to aircraft measurements at lower elevations). It can be seen that these two profiles are similar.

The similarity of the two sets of profiles in Figure 8 is a matter of interest in itself: the carbon-14 concentrations averaged to 30°N

along lines equi-distant above the standard, sloping tropopause are very nearly the same as the actual concentrations at 30°N. A one-dimensional, vertical, eddy-diffusion model located at 30°N is, in this sense, an approximate model for the northern hemisphere.

CALIBRATION OF ONE-DIMENSIONAL MODELS AGAINST OBSERVED CARBON-14 DATA.

The profiles of excess carbon-14 for January 1963 were extended to the surface of the earth on the basis of observed carbon-14 in the troposphere, and it was extended from the observed point of highest elevation to 50 km by a decreasing exponential function. This extended mixing ratio profile was used as the initial condition for calculations using the various K_z functions. The vertical grid was every kilometer from 0 to 50. The lower boundary condition was that observed at 1 kilometer, which remained constant for several years near 3×10^{-16} mixing ratio. The upper boundary condition was that the concentration at 51 km was one-half that at 50 km. The vertical eddy diffusion problem was set up in terms of first-order differencing, which guarantees conservation of mass even with the non-continuous K_z functions of Figure 2. The problem was thus one of 50 simultaneous linear equations with constant coefficients. The problem was solved by the Gear method (Hindmarsh, 1972) on the Lawrence Berkeley Laboratories CDC 7600 computer. With the boundary conditions specified, with the initial profile specified, and with use of a given K_z function, it was a simple matter to compute the predicted carbon-14 distribution at any future time. Typically the future profiles were calculated every 3 months for two years and then every year to a

total of 10 years. These calculated profiles, for each K_z function, are then compared with the observed ones. This procedure was repeated with the initial distribution taken to be April 1963 instead of January 1963, also July 1963, January 1964 and January 1965.

These calculations were made for the seven K_z functions shown in Figure 2 and for Brasseur's (1972) "K-max" and "K-min", all of which are listed in Table A1 of the appendix. We have made a large number of plots of calculated profiles and observed profiles for the nine K_z functions. Four sets of these plots are given by Figures 9, 10, 11 and 12. Each of these plots is of special interest for one reason or another, and each is discussed below.

In Figure 9, the initial profile is that of January 1963 and the predicted profiles are January 1964. This period is of interest in that it represents the case of maximum gradients, and the sharpest initial distribution. There was a substantial change in one year in the northern hemisphere profile, and there was relatively little loss to the southern hemisphere. The different K_z models give strongly different predictions, one relative to another. The predictions of the models will be discussed below.

In Figure 10, the initial profile is that of January 1964 and the observed points are from the balloon measurements directly observed at 30°N in January 1966. Again, there are strong differences in prediction by the 9 models; and the sense of the differences is the same in Figure 10 as in Figure 9.

In Figure 11, the initial profile is that observed locally by balloon in January 1965 and the observed data are those obtained directly

by balloon in December 1970. On January 1965, 66 percent of the stratospheric carbon-14 was in the northern hemisphere and 34 percent was in the southern hemisphere, but in December 1970 it was essentially equal in the two hemispheres (Table 2). This transport to the southern hemisphere was allowed for, as follows: the magnitude of the initial condition was taken to be the average between the northern and southern hemispheres, rather than the actual value in the northern hemisphere. From consideration of Table 2 the actual concentrations of January 1965 were reduced by the factor 0.75. The observed carbon-14 in November 1970 is spread between 20 and 35 km, with a maximum mixing ratio at about 25 km. There were French and Chinese atmospheric tests of nuclear bombs between 1967 and 1970. According to Telegadas et al (1972), the 1967-70 tests inserted radioactive debris between 14 and 18 km in the northern hemisphere and between 15 and 19 km in the southern hemisphere, and they stated that the carbon-14 above 20 km in December 1970 was primarily contributed by the bomb-test series that ended in December 1962.

The predictions of the nine K_z functions are compared with each other and with observed carbon-14 distributions in Figures 9, 10, and 11. Similar comparisons were made with other observed carbon-14 distributions taken as the initial values and with all later observed carbon-14 distributions taken as comparison for predicted versus observed profiles. The pattern shown by Figures 9-11 is confirmed by all of these comparisons, but Figure 12 gives the example that departs the most from the general pattern. This figure gives the poorest agreement between observed profiles and those calculated by Hunten's model.

DISCUSSION

The excess carbon-14 cloud, spread over the northern hemisphere by the atmospheric nuclear bomb test series of 1961-62, appears to provide a useful calibration for theories of stratospheric motions. The observations of carbon-14 provide direct data for large-scale stratospheric sweep-out times in the region 15 to 25 kilometers.

The vertical eddy-diffusion functions, K_z, were derived by the various authors from considerations of: (1) heat flux data; (2) vertical profiles of ozone; (3) vertical profiles of methane; (4) radioactive fall-out from nuclear bomb tests, primarily involving particulate tracers such as strontium-90, tungsten-185, etc. (5) other considerations. It appears that no one made detailed use of the carbon-14 data. Thus this study is an independent test of the models.

The nine models using vertical eddy diffusion constants K_z as a function of height give markedly different predictions, one relative to another, concerning the dissipation of the carbon-14 cloud during the period 1963-70. The relative and absolute predictions made by the nine K_z models are very nearly the same for the four time intervals of Figures 9-12.

Figure	Time interval
9	Jan. 1963 - Jan. 1964
10	Jan. 1964 - Jan. 1966
11	Jan. 1965 - Nov. 1970
12	April 1963 - Jan. 1965

The model associated with an investigator is often not the only model considered by the investigator. For example, Crutzen has used several

other K_z models; and he has used a different, preferred model in recent calculations. The model associated with Whitten is an early one that he considered and rejected; it is retained here as an extreme example not as a test of Whitten's recent work. For the present purpose, it is necessary to adhere to these models, even if they do not represent the investigators latest, best judgment, because these models were used in Chang's (1974) comparative study (Figure 1B) of the effect of model on SST perturbation, and it is desirable to compare predictions of carbon-14 with those for the SSTs. Crutzen's model used here is valuable in showing the effect of K_z constant with height in the stratosphere. Whitten's model is of interest in showing what a large difference in stratospheric sweep-out time is caused by differences in K_z function, Figure 2. Brasseur's "K-min" shows the effect of a very low K_z value high in the stratosphere. McElroy's or Hunten's model shows the effect of a region of low K_z low in the stratosphere. Chang's model shows the effect of a region of low K_z in the mid stratosphere.

The models with large values of K_z at all heights, such as Brasseur's K-max or Whitten's function, sweep excess carbon-14 out of the stratosphere very much faster than that observed. This discrepancy is so large that line 7 should be dropped from Figure 1B in any realistic discussion of SSTs.

Chang's model has minimum K_z at 30 km and Brasseur's "K-min" has minimum K_z at 37 km. These models sweep out the region 17 to 21 km at much too fast a rate, but these models build up relatively large mixing ratios near 35 km over a long period of time. Chang's peak mixing ratio at 35 km in Figure 11 agrees with the observed carbon-14, but Brasseur's "K-min"

retains too much carbon-14 at 35 km. If there was a large hidden source of carbon-14 above 35 km in 1963, then Chang's model would greatly overpredict the amount of carbon-14 at 35 km in November 1970 (Figure 11).

Except for the discontinuity at 10 km in the troposphere, Crutzen's K_z function is constant with height. It sweeps out the region around 20 km much faster than was observed, and it gives a long-term profile (Figure 11) of a shape rather different from that observed. A change of the absolute value of K_z can give approximately correct sweep-out times near 20 km, but the shape of the profile is not improved.

Four functions (5, Stewart; 6, McElroy; 8, Shimazaki, and 12, Hunten) are qualitatively similar: large K_z in the troposphere, minimum K_z in the lower stratosphere, and increasing K_z with height from lower to upper stratosphere. They differ largely as to height of tropopause, height of minimum K_z, and magnitude of K_z at the minimum. The relatively small differences in these K_z functions (Figure 2) lead to substantial differences in predicted history of carbon-14 in the stratosphere. The height of Shimazaki's region of small K_z is too low (note the low elevation of peak carbon-14 in Figures 9 and 10), and the average value of his K_z appears to be too large (note the almost totally swept out stratosphere by 1970). Stewart's model gives a fairly good representation of the shape of the carbon-14 profile and very nearly the correct height of maximum carbon-14 in the various comparisons; but the magnitude of his K_z function between 15 and 25 km appears to be too large, because it always predicts too little carbon-14 in the stratosphere. McElroy's function gives many predictions in approximate agreement with observations (his function is best for the interval January 1964 to January 1965); but the tropopause

is about 2 kilometers too high; and this K_z function appears to be too large on the average since it has swept too much carbon-14 out of the stratosphere over the long period of time (Figure 11).

Hunten's model of K_z gives a reasonably correct prediction of the shape, elevation of the maximum, and magnitude of the carbon-14 cloud for all tested initial and final profiles. Figure 12 gives the worst predictions found using Hunten's model. This model appears to be superior to other models tested here. However, even this model somewhat underestimates the persistence of carbon-14 after eight years, Figure 11.

We have explored the effects of introducing small changes in some of the models. The long-term predictions of the carbon-14 distribution are very sensitive to small perturbations of assumed K_z. The predictions are strongly dependent on both the shape and the magnitude of the K_z function. The long-term, carbon-14, peak-concentration near 20 km (Figure 10, for example) appears to require the qualitative features of McElroy's or Hunten's model, that is, low values between 15 and 20 km and rapidly increasing values above 25 km.

In view of the considerable success of Hunten's model in describing the carbon-14 data, it is of interest to examine the full predictions of his model for the eight year period, taking the initial distribution as of January 1963. In terms of mixing ratios from 0 to 50 km, these predictions are given for January 1964, January 1965, January 1966, and November 1970, Figure 13. The lower boundary value was taken to be 2.8×10^{-16} at all times. The upper boundary value is that the concentration at 51 km is half that at 50 km. For each calculated profile, the initial

distribution of January 1963 was reduced to correct for subsequent transport of carbon-14 to the southern hemisphere. For example, the initial distribution of January 1963 was reduced by the factor .66/.87 for the calculated curve for January 1965 (note the column in Table 2, % N.H.). The triangles are direct observations at 30°N and the circles are the specially defined northern hemisphere average. This K_z function is fairly successful in predicting the history of the carbon-14 over the eight-year period. The terminal prediction for November 1970 is very similar for January 1963 as initial state (Figure 12) as for January 1965 as initial condition (Figure 11). This agreement of terminal prediction, regardless of initial time, is regarded as evidence against a large pocket of carbon-14 above the polar region causing the separation of carbon-14 and strontium-90 in Figure 6.

There is a strong correlation between the correctness of predicting the carbon-14 profile in Figures 9 and 10 (but not so much so for the long-term case of Figure 11) and the magnitude of the reduction of ozone by the SST perturbation, Figure 1B. In Figures 9 and 10, the best predictions of carbon-14 are made by Hunten, Stewart, and McElroy; and in Figure 1B these predict the three largest reductions of ozone by SSTs. Crutzen, Chang, and Shimazaki give comparable predictions of carbon-14 in Figures 9 and 10, and they give about the same magnitude of ozone depletion, which is about a factor of two less than the Hunten-McElroy-Stewart group. However, the predicted ozone reduction by SSTs is less sensitive to the K_z function than is the sweep-out of the cloud of carbon-14.

Finally, it is of interest to consider the reduction of ozone as a function of added NO_x, using Hunten's K_z function, Chang's calculation with Hunten's K_z function (Figure 1B), and Grobecker's (1974) projected injection of NO_x (This projection applies if there is no reduction of the NO_x emission index from supersonic transports). Grobecker's projected upper bound NO_x injections at both 17 km (15 to 18) and at 20 km (18 to 21) are given in Table 3. Grobecker's (1974) upper bound NO_x and Chang's (1974) one-dimensional photochemical model with Hunten's (1974) K_z function give very large reductions of global ozone, substantially greater than a factor of two after the year 2010 (Table 3).

ACKNOWLEDGEMENT

This work was supported by the Climatic Impact Assessment Program by means of an interagency agreement between the Department of Transportation and the Atomic Energy Commission through the Inorganic Materials Research Division, Lawrence Berkeley Laboratory. We wish to express our appreciation to James Friend, a co-author of the paper by Seitz et al (1968), who suggested the idea of averaging the carbon-14 data along non-horizontal lines.

TABLE 3

GLOBAL PROJECTIONS OF NO_x INSERTION (UNITS OF 10^{12} g NO_2 yr^{-1}) AT 17 KM AND AT 20 KM (GROBECKER, 1974) AND OZONE REDUCTION AS CALCULATED BY CHANG (1974) USING HUNTEN'S K_z FUNCTION (1974)

Year	NO_x insertion		Per cent ozone depletion from NO_x inserted at:		
	17 km	20 km	17 km	20 km	Total
1990	.45	.22	3.0	2.5	5.5
1996	.60	1.3	4.0	13	17
2000	.70	3.0	4.5	23	27
2006	1.0	6.5	6.2	37	33
2010	1.1	9.0	6.7	43	49
2015	1.2	12	7.2	47	54
2020	1.5	20	8.7	52	61
2025	1.6	27	9.2	60	69

REFERENCES

Brasseur, G., Stratospheric chemistry, Aeronomica Acta, B41, Institute d' Aeronomie Spatiale de Belgique, Brussels, 1972.

Chang, J. S., Simulations, perturbations, and interpretations, paper presented at the Third CIAP Conference, Cambridge, Mass., Feb. 26-Mar. 4, 1974.

Chang, J. S., Fourth CIAP Conference, Cambridge, Mass., February 1975.

Crutzen, P., A review of upper atmospheric photochemistry, Can. J. Chem. 52, 1569-1581, 1974.

Cunnold, D. M., F. N. Alyea, N. A. Phillips, and R. G. Prinn, First results of a general circulation model applied to the SST-NO_x problem, Paper presented at a meeting of the AMS/AIAA Second International Conference on the Environmental Impact of Aerospace Operations in the High Atmosphere, San Diego, Calif., July 8-10, 1974.

Grobecker, A. J., Research program for assessment of stratospheric pollution, Acta Astron., 1, 179-224, 1974.

Hagemann, F. T., J. Gray, Jr., and L. Machta, Carbon-14 measurements in the atmosphere - 1953 to 1964. Health and Safety Laboratory Report 159, U.S. Atomic Energy Commission, p. 11 (1965).

Hard, T. M., Stratospheric trace-gas measurements, Technical Report, Transportation Systems Center, Cambridge, Mass., November 1974.

Hindmarsh, A. C., Gear: Ordinary differential equation system solver, Lawrence Livermore Laboratory Report UCID-30001, Rev. 1, 1972.

Hesstvedt, E., Proc. of the Int. Conf. on Structure, Composition, and General Circulation of the Upper and Lower Atmospheres and Possible Anthropogenic Perturbations, Melbourne, Australia, 1097-1106.

Hunten, D. M., Stratospheric pollution and how it dissipates, submitted to Science, 1974.

Johnston, H. S., Reduction of stratospheric ozone by nitrogen oxide catalysts from supersonic transport exhaust, Science 173, 517-522; Catalytic reduction of stratospheric ozone by nitrogen oxides, UCRL Report No. 20568, 1-106, 1971.

Johnston, H. S., G. Whitten, and J. Birks, The effect of nuclear explosions on stratospheric nitric oxide and ozone, J. Geophys. Res. 78, 6107-6135, 1973.

McElroy, M., S. Wofsy, J. Penner, J. McConnell, Atmospheric ozone: Possible impact of stratospheric aviation, J. Atmospheric Sci., 31, 287-300, 1974.

Shimazaki, T., and T. Ogawa, Theoretical models of minor constituents' distributions in the stratosphere and the impacts of the SST exhaust gases, Paper presented at the IAMAP/IAPSO First Special Assemblies, Melbourne, Australia, 1974.

Seitz, H., B. Davidson, J. P. Friend, and H. W. Feeley, Numerical models of transport, diffusion, and fallout of stratospheric radioactive material. Final report on project Streak. Report No. NYO-3654-4. Isotopes - A Teledyne Company, 50 van Buren Avenue, Westwood, New Jersey (May 1968).

Stewart, R., Response of stratospheric ozone to the simulated injections of nitric oxide, American Geophysical Union, Fall Meeting, San Francisco, California, December 1973.

Telegadas, K., J. Gray, Jr., R. E. Sowl, and T. E. Ashenfelter, Carbon-14 measurements in the stratosphere from a balloon-borne molecular sieve sampler. Health and Safety Laboratory Report 246, U.S. Atomic Energy Commission, 69-106, 1972.

Telegadas, K., The seasonal stratospheric distribution of Cadmium-109, Plutonium-238, and Strontium-90, Health and Safety Laboratory Report-184, U.S. Atomic Energy Commission, 53-118, 1967.

Telegadas, K., The seasonal stratospheric distribution and inventories of excess carbon-14 from March 1955 to July 1969, Health and Safety Laboratory Report-243, U.S. Atomic Energy Commission, 3-86, 1971.

Telegadas, K., and R. J. List, Are particulate radioactive tracers indicative of stratospheric motions, J. Geophys. Res., 74, 1339-1350, 1969.

Vupputuri, R. K., The role of stratospheric pollutant gases (H_2O, NO_x) in the ozone balance and its implications for the seasonal climate of the stratosphere, Paper presented at the IAMAP/IAPSO First Special Assemblies, Melbourne, Australia, 1974.

Whitten, R. C., and R. P. Turco, The effect of SST emission on the earth's ozone layer, paper presented at the IAMPA/IAPSO First Special Assemblies, Melbourne, Australia, 1974.

APPENDIX

Tables A1, A2, A3, A4, A5, A6

TABLE A1

VERTICAL EDDY DIFFUSION FUNCTION K_z

(IN UNITS OF 10^3 cm^2 sec^{-1})

Kilometers

1	2	3	4	5	6	7	8	9	10
11	12	13	14	15	16	17	18	19	20
21	22	23	24	25	26	27	28	29	30
31	32	33	34	35	36	37	38	39	40
41	42	43	44	45	46	47	48	49	50

Hunten

100.	100.	100.	100.	100.	100.	100.	100.	100.	30.
30.	30.	30.	2.3	2.3	2.7	3.0	3.3	3.7	4.2
4.5	5.2	5.6	6.4	7.2	8.0	9.0	10.	11.	12.
13.	15.	16.	18.	20.	22.	24.	28.	30.	34.
38.	41.	47.	52.	59.	63.	72.	80.	90.	100.

Chang

300.	300.	300.	300.	300.	300.	300.	300.	300.	300.
23.	18.	15.	12.	11.	9.7	8.6	7.4	6.6	6.0
5.3	5.0	4.5	4.2	4.0	3.9	3.7	3.7	3.7	3.7
3.8	3.9	4.0	4.2	4.5	5.0	5.4	6.1	7.0	8.0
9.2	11.	13.	15.	18.	22.	26.	33.	42.	54.

Stewart

300.	300.	300.	300.	270.	220.	150.	90.	42.	23.
13.	8.2	6.0	5.1	5.0	5.1	5.2	5.4	5.6	6.0
6.2	6.6	7.0	7.3	7.8	8.2	8.9	9.1	9.9	11.
12.	13.	14.	15.	16.	18.	20.	22.	26.	30.
33.	40.	45.	56.	66.	78.	93.	120.	140.	160.

Whitten

100.	100.	100.	100.	100.	100.	100.	100.	100.	44.
42.	40.	38.	35.	34.	32.	31.	28.	27.	26.
25.	23.	22.	21.	20.	19.	18.	17.	16.	15.
15.	14.	14.	14.	14.	14.	15.	16.	17.	18.
20.	22.	25.	3.0	35.	42.	56.	75.	100.	130.

Shimazaki

100.	100.	100.	100.	100.	100.	100.	100.	100.	6.4
7.0	7.5	8.1	8.9	9.2	10.	11.	12.	13.	14.
14.	15.	16.	17.	18.	20.	23.	24.	25.	27.
29.	31.	33.	35.	39.	42.	44.	48.	51.	55.
6.0	63.	69.	73.	80.	85.	91.	99.	110.	120.

McElroy

300.	300.	300.	300.	300.	300.	300.	300.	300.	300.
300.	300.	300.	300.	300.	2.0	2.0	2.0	4.0	7.0
9.0	12.	15.	19.	22.	25.	30.	35.	40.	45.
52.	59.	65.	7.2	81.	90.	9.9	110.	120.	130.
140.	150.	160.	170.	180.	200.	220.	230.	240.	260.

Crutzen

300.	300.	300.	300.	300.	300.	300.	300.	300.	300.
10.	10.	10.	10.	10.	10.	10.	10.	10.	10.
10.	10.	10.	10.	10.	10.	10.	10.	10.	10.
10.	10.	10.	10.	10.	10.	10.	10.	10.	10.
10.	10.	10.	10.	10.	10.	10.	10.	10.	10.

Brass Min.

190.	180.	170.	150.	140.	130.	120.	98.	82.	70.
58.	45.	38.	31.	25.	21.	18.	14.	12.	10.
8.1	6.5	5.5	4.3	3.4	2.8	2.3	1.9	1.5	1.3
1.1	.80	.75	.62	.54	.51	.51	.52	.54	.58
.65	.74	.83	.95	1.1	1.2	1.4	1.7	2.0	2.2

Brass Max.

190.	180.	170.	160.	150.	145.	140.	135.	130.	127.
124.	120.	115.	110.	98.	91.	84.	78.	71.	64.
60.	53.	48.	43.	38.	34.	30.	26.	23.	22.
20.	17.	15.	14.5	14.	14.	14.	14.5	15.	16.
17.	18.	21.	22.	23.	25.	28.	32.	34.	38.

TABLE A2.A

MIXING RATIOS (V/V) OF EXCESS CARBON-14 AT 30°N

(MULTIPLES OF 10^{-16}), BASED ON DIRECTLY OBSERVED LOCAL VALUES.

KM	1/63	4/63	7/63	10/63	1/64	1/65	1/66
36							
35							
34							
33			20.6	18.5	16.9	12.1	14.3
32	7.58	9.55					
30			24.0	23.8	19.2	21.4	14.1
27		20.2	22.1	26.7	20.2	18.0	14.1
26	9.60						
25	10.0	33.6		44.6			
24		35.5	39.8		30.7	22.4	16.7
22							
21							
20	77.1	59.4	46.8	55.1	40.4	24.9	15.0
19	73.0		43.8			18.3	14.2
18	55.7	40.2	33.6	30.9	31.7	14.3	
15	20.8	9.84	5.23	8.48	7.54	4.85	
12	5.81	11.3	3.02	3.36	3.98	3.93	
8	2.92	3.79	3.12	2.98	3.60	3.17	
4	2.98	3.12	2.93	2.93	3.65	2.93	
0		2.10	2.91	2.77	2.84	2.75	

TABLE A2.B

CARBON-14 MIXING RATIOS α AS OBSERVED AT VARIOUS LATITUDES AND HEIGHTS (MULTIPLES OF 10^{-16}), JANUARY 1966

9°N		30°N		70°N	
km	α	km	α	km	α
4.5	2.84	4.5	3.18	1.0	3.18
8.5	2.80	8.3	2.99	4.3	3.08
12.0	2.99	11.8	3.42	7.5	3.18
14.8	3.13	15.0	4.34	11.9	7.04
18.0	3.90	16.2	11.7	15.0	13.0
19.0	4.58	17.8	13.4	17.8	16.1
19.5	4.63	18.8	17.1	18.5	15.3
		19.0	14.2	18.8	19.4
		19.5	15.0	19.2	18.4
		24.0	16.7		
		27.2	14.1		
		30.0	14.1		
		31.0	15.8		
		32.8	14.3		

TABLE A2.C

CARBON-14 MIXING RATIOS α OBSERVED BY BALLOON AND CONTOUR LINES AS INFERRED FROM BALLOON PLUS AIRCRAFT SAMPLING (MULTIPLES OF 10^{-16}). NOVEMBER 1970.

9°N	
km	α
20.8	3.71
21.0	3.86
21.4	4.34
22.0	4.82
23.0	5.30
23.7	5.78
27.2	5.35
30.6	5.30
31.5	5.11

34°S	
km	α
20.0	5.78
20.9	5.74
21.1	6.17
21.7	6.27
23.9	6.27
24.2	6.51
27.0	6.46
27.2	6.27
27.3	5.78
32.3	5.78

30°N	
km	α
19.6	5.30
20.3	5.78
21.0	6.51
21.2	6.17
22.2	6.27
23.9	6.84
24.3	6.75
24.4	6.70
26.5	6.75
27.2	6.31
27.6	6.84
31.2	6.27
32.5	5.59
32.8	6.17
33.0	6.27
34.0	5.78
35.5	5.30
36.3	4.63

42°N	
km	α
19.6	5.78
20.9	6.03
21.3	6.27
23.3	6.75
24.0	6.89
27.2	6.75
27.4	6.65
30.8	6.46
31.5	6.27
36.0	6.03

65°N	
km	α
20.3	6.27
22.3	6.75
24.0	6.70
26.9	6.80
27.0	6.75
30.0	6.27
31.0	5.78

TABLE A3.A

CONCENTRATION OF EXCESS CARBON-14 (10^3 MOLECULES CM^{-3})

January 1963

KM.	80°N	70°N	60°N	50°N	40°N	30°N	20°N	10°N	0°N	10°S	20°S	30°S
29								0.3	0.3	0.3		
28							0.4	0.5	0.5	0.5	0.4	
27						0.4	0.6	0.6	0.6	0.6	0.6	0.4
26					0.6	0.6	0.8	0.8	0.8	0.8	0.8	0.6
25				0.8	0.8	0.8	1.0	1.4	1.2	1.0	0.8	0.8
24		0.9	1.0	1.2	1.0	1.4	2.8	3.0	1.6	1.2	1.0	0.8
23	1.2	1.2	1.4	1.6	2.0	5.6	6.4	4.2	1.8	1.2	1.0	1.0
22	1.8	1.8	2.8	4.4	9.4	11.6	10.4	4.4	1.8	1.4	1.2	1.0
21	3.8	5.6	10.2	12.0	15.8	14.8	12.2	4.2	1.8	1.6	1.2	1.0
20	12.6	13.4	16.4	18.4	18.2	16.4	12.6	3.6	1.6	1.4	1.2	1.2
19	19.4	20.6	20.8	21.4	18.6	16.0	11.4	3.0	1.4	1.4	1.4	1.2
18	25.0	25.2	24.8	22.8	17.0	14.8	6.8	2.2	1.2	1.2	1.4	1.2
17	30.4	28.6	27.0	21.2	15.2	12.2	5.8	1.4	1.2	1.0	1.4	1.2
16	33.6	30.6	25.0	19.2	13.0	9.2	5.0	1.2	1.0	1.0	1.4	1.4
15	32.8	28.2	22.0	16.4	10.8	7.4	4.2	1.0	0.8	0.8	1.2	1.2
14	28.8	23.8	18.0	12.0	8.8	6.4	3.6				1.2	1.2
13	21.4	16.0	12.6	9.2	6.2	5.4						1.2
12	14.0	11.6	9.8	6.2	3.6							
11	11.4	9.8	4.6	3.4								
10	9.8	7.6	4.0									
9	8.0	4.2										
8	4.4											

TABLE A3.B

January 1964

KM.	80°N	70°N	60°N	50°N	40°N	30°N	20°N	10°N	0°	10°S	20°S	30°S
29								0.9	0.9	0.9		
28							1.0	1.0	0.9	0.9	0.8	
27						1.2	1.2	1.1	1.0	1.0	0.8	0.7
26					1.6	1.6	1.8	1.2	1.3	1.0	0.8	0.8
25				2.1	2.2	2.4	2.4	1.5	1.6	1.2	0.9	0.8
24			2.6	2.8	3.2	3.2	3.4	2.0	1.7	1.4	0.9	0.9
23		3.2	3.6	3.8	4.4	4.6	4.6	3.4	1.8	1.6	1.0	0.9
22	4.2	4.4	4.8	5.2	5.6	6.0	5.6	3.8	1.9	1.6	1.1	1.0
21	5.4	6.0	6.6	7.0	7.8	7.4	6.4	3.6	1.9	1.6	1.2	1.1
20	7.2	7.6	8.2	8.6	8.6	8.2	6.6	3.4	1.8	1.6	1.1	1.1
19	9.0	9.0	10.0	9.4	9.4	8.8	6.4	2.8	1.8	1.4	1.1	1.0
18	11.4	10.8	11.0	10.2	10.0	8.2	5.4	2.4	1.8	1.4	1.0	1.0
17	13.0	12.0	11.2	11.0	9.6	7.2	3.2	2.0	1.7	1.4	1.0	1.0
16	14.2	12.2	9.2	10.2	9.0	4.8	2.3	1.7	1.6	1.4	1.2	1.1
15	14.8	13.0	11.4	6.8	9.0	3.4	1.9	1.6	1.6	1.4	1.3	1.2
14	15.2	13.8	12.6	7.8	10.4	3.4	1.8				1.5	1.4
13	14.6	13.0	11.6	8.2	8.4	2.6						
12	13.0	12.0	8.8	2.4	4.0							
11	11.2	10.4	6.2	3.0								
10	9.6	7.0	4.4									
9	7.6	5.4										
8	5.8											

TABLE A3.C

January 1965

KM.	80°N	70°N	60°N	50°N	40°N	30°N	20°N	10°N	0°	10°S	20°S	30°S
29								0.9	0.5	0.5		
28							1.2	1.0	0.6	0.6	0.5	
27						1.6	1.4	1.2	0.8	0.8	0.6	0.7
26					1.5	1.8	1.8	1.4	1.0	1.0	0.8	0.8
25				2.0	1.8	2.1	2.0	1.7	1.2	1.2	1.0	0.9
24			2.0	2.2	2.2	2.4	2.4	2.0	1.4	1.4	1.2	1.0
23		2.4	2.4	2.7	2.6	2.8	2.8	2.4	1.7	1.7	1.5	1.2
22	3.0	2.8	2.9	3.2	3.2	3.4	3.2	2.6	2.0	2.0	1.8	1.4
21	3.4	3.3	3.4	3.6	3.8	3.9	3.8	2.7	2.4	2.2	2.0	1.7
20	4.0	3.8	4.0	4.2	4.4	4.4	3.8	2.6	2.6	2.4	2.2	1.9
19	4.6	4.6	4.8	5.2	5.0	4.4	3.4	2.6	2.3	2.2	2.3	2.0
18	5.4	5.4	5.6	5.8	5.0	3.8	2.6	1.2	1.4	1.4	1.8	1.8
17	6.0	5.8	5.9	5.4	4.4	3.0	1.6	1.0	0.8	0.9	1.3	1.6
16	6.3	6.0	5.8	5.2	3.4	1.8	1.4	1.0	0.9	1.0	1.0	1.4
15	6.3	6.0	5.8	4.0	2.6	1.4	1.2	1.1	1.1	1.2	1.0	1.2
14	6.0	6.0	5 .2	2.6	2.2	1.6	1.2				1.0	1.0
13	5.7	4.8	4.0	2.5	2.1	1.7						1.0
12	5.4	4.4	3.6	2.4	2.2							
11	5.0	4.0	3.4	2.6								
10	4.6	3.8	3.2									
9	4.2	3.4										
8	4,0											

TABLE A4

RELATIVE MIXING RATIO* OF STRONTIUM-90 AT 30°N

April 1963		July 1963		October 1963		Jan. 1964		Jan. 1965		Jan. 1966	
KM	$^{90}S_R$	KM	$^{90}S_R$	KM	$^{90}S_R$	KM	$^{90}S_R$	KM	$^{90}S_R$	KM	$^{90}S_R$
30.3	200	29.0	300	32.0	200	29.5	100	30.3	30	32.5	10
28.0	500	28.0	400	28.5	300	26.5	200	26.8	50	29.8	20
24.3	1000	26.5	500	26.5	500	25.2	300	25.2	100	28.2	30
23.2	1500	23.9	1000	23.7	1000	23.6	500	21.8	200	27.0	40
21.8	1700	22.8	1500	21.9	1200	22.4	800	21.4	300	26.0	50
19.3	1700	21.8	1700	21.2	1500	21.6	900	20.9	350	24.6	100
18.5	1500	19.2	1700	19.4	1500	20.6	1000	19.2	350	22.2	150
17.7	1000	18.6	1500	19.1	1200	19.2	1000	17.9	300	20.0	150
16.2	500	17.8	1000	18.5	1000	18.7	900	16.7	200	18.3	130
14.0	200	16.5	500	17.2	500	18.3	800	16.2	100	17.8	100
10.8	100	16.0	200	16.2	300	17.2	500	15.8	50	17.0	50
9.5	50	15.5	100	15.8	200	16.2	300	14.0	10	12.0	10
7.3	26	14.9	50	15.6	100	15.7	200				
6.0	14	14.1	10	15.2	50	13.5	100				
4.5	7			14.0	10	12.0	50				
						10.5	22				

*In Units of Disintegrations per Minute per 1000 Cubic Feet of Standard Air.

TABLE A.5

AVERAGE CONCENTRATION OF EXCESS CARBON-14 AT 30°N

(UNITS OF 10^3 ATOMS CM^{-3})

KM	1/63	4/63	7/63	10/63	1/64	1/65
27	0.61	1.38	2.09	2.14	1.58	1.48
26	0.89	2.08	2.52	2.84	2.05	1.70
25	1.72	3.11	3.42	3.75	2.80	2.07
24	3.69	4.65	4.71	4.87	3.70	2.40
23	7.76	6.77	6.45	6.19	4.81	2.85
22	11.9	9.91	8.71	7.75	6.11	3.36
21	14.6	11.9	9.98	8.92	7.13	3.89
20	15.7	12.6	10.0	9.37	7.70	4.31
19	14.8	11.4	9.07	9.12	7.85	4.28
18	13.1	10.1	8.07	8.02	7.76	4.03
17	10.1	9.10	7.95	6.73	6.88	3.35
16	7.7	8.44	7.30	5.19	6.00	2.28
15	6.25	7.85	6.16	4.50	5.40	1.96
14	4.59	6.00	4.77	3.71	3.86	1.90
13	3.25	4.47	3.73	3.17	2.87	1.94

TABLE A.6

MIXING RATIOS (V/V) OF EXCESS CARBON-14 AT 30°N

(MULTIPLES OF 10^{-16}), BASED ON AVERAGE VALUES FROM TABLE A5.

KM	1/63	4/63	7/63	10/63	1/64	1/65
27	10.2	22.9	34.5	35.4	26.2	24.4
26	12.5	29.3	35.6	40.1	28.9	24.0
25	20.7	37.4	41.1	45.0	33.6	24.8
24	38.3	48.4	49.0	50.6	38.4	24.9
23	67.0	58.5	55.7	53.4	41.6	24.6
22	87.6	72.6	63.8	56.7	44.7	24.6
21	90.9	74.2	62.0	55.4	44.3	24.1
20	82.8	66.5	53.1	49.3	40.6	22.7
19	66.3	51.3	40.5	40.8	35.1	19.1
18	49.8	38.4	30.7	30.5	29.5	15.3
17	32.9	29.5	25.8	21.8	22.3	10.8
16	21.6	23.4	20.2	14.4	16.6	6.3
15	14.9	18.7	14.7	10.7	12.8	4.6
14	9.4	12.3	9.8	7.6	7.9	3.9
13	5.8	8.0	6.6	5.6	5.1	3.4

TITLES TO FIGURES

1. Calculated percentage reduction of the average global ozone column as a function of the mass of NO_x inserted at 20 km.

   A. Results available for each of twelve different groups.

   B. Seven one-dimensional models of vertical eddy diffusion function K_z were recalculated on a uniform basis by Chang (1974). The upper limit of NO_x insertion is the upper bound projected by Grobecker (1974) for the year 2025.

   The modelers are identified by the number code: (1) Johnston, 1971; (2) Crutzen, 1974; (3) Hesstvedt, 1974, 2D model; (4) Chang, 1974; (5) Stewart, 1973; (6) McElroy et al, 1974; (7) Whitten and Turco, 1974; (8) Shimazaki and Ogawa, 1974; (9) Vupputuri, 1974, 2D model; (10) Widhopf, 1974, 2D model; (11) Cunnold et al, 1974, 3D model; (12) Hunten, 1974.

2. Vertical eddy diffusion functions, K_z, for seven one-dimensional modelers: Numbered as in Figure 1. (A, B) Brasseur, 1972.

3. Relative mixing ratios (10^5 atoms of excess carbon-14 per gram of air) of excess carbon-14 as measured by balloons and U-2 aircraft. The data were taken during the period March-May 1963 and are referred to as April 1963. Telegadas, 1971.

4. Concentration of excess carbon-14 (units of 10^3 molecules cm^{-3}) for the indicated times. These zonal-average maps of ^{14}C concentration were derived from mixing ratio maps such as Figure 3.

5. Relative mixing ratios (disintegrations per minute per 1000 cubic feet of standard air) of strontium-90 for April 1963. Telegadas, 1967.

TITLES TO FIGURES (CONTINUED)

6. Comparison of observed strontium-90 (solid line) and excess carbon-14 mixing ratios normalized to 21 km, April 1963.

7. Northern hemispherical average (see text) concentration of excess carbon-14 as a function of height between January 1963 and January 1965. These averages are ascribed to the geographical average of the northern hemisphere, namely 30°N.

8. Comparison of average (Figure 7) mixing ratios and locally observed (balloon soundings) mixing ratios of excess carbon-14 at 30°N.

   ○, hemispherical average

   △, local observation at 30°N

9. Comparison of average observed excess carbon-14 on January 1964 with that calculated by nine models of K_z (Figure 2, Table A1) for January 1964. The initial distribution for calculation was the observed distribution for January 1963. Both initial and final conditions correspond to ○ in Figure 8.

10. Comparison of directly observed excess carbon-14 on January 1966 with that calculated by nine models of K_z for January 1966. The initial distribution for each computation was the observed distribution on January 1964. (In terms of Figure 8: ○, 1964; △, 1966).

11. Comparison of directly observed carbon-14 mixing ratios on November 1970 with that calculated by nine models of K_z for January 1971. The initial distribution for each computation was the global average, observed distribution on January 1965. According to Telegadas et al

TITLES TO FIGURES (CONTINUED)

(1972), this excess carbon-14 was left over from the 1961-62 test series, and it was not a part of the 1967-70 series of relatively small bombs, which deposited their debris in the stratosphere between 14 and 18 km. (In terms of Figure 8: △, 1965; △, 1970.

12. Comparison of average observed excess carbon-14 on July 1963, October 1963, and January 1965 with initial conditions based on April 1963.

13. Calculated and observed excess carbon-14 mixing ratios in the stratosphere one, two, three, and eight years after January 1963 (corrected for transport to southern hemisphere). The curves were calculated by Hunten's model. ○, ● northern hemisphere average; △, ▲ direct observation at 30°N.

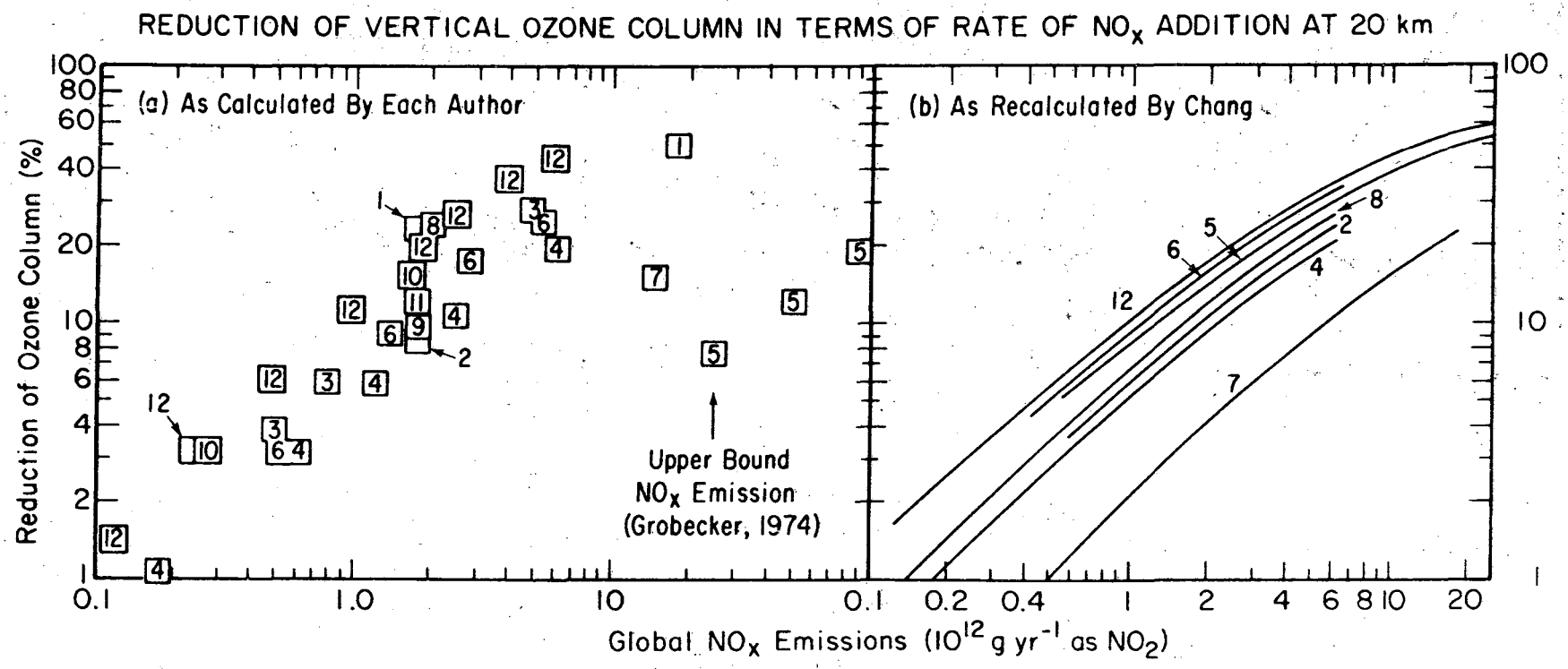

FIGURE 1

XBL-7412-7639

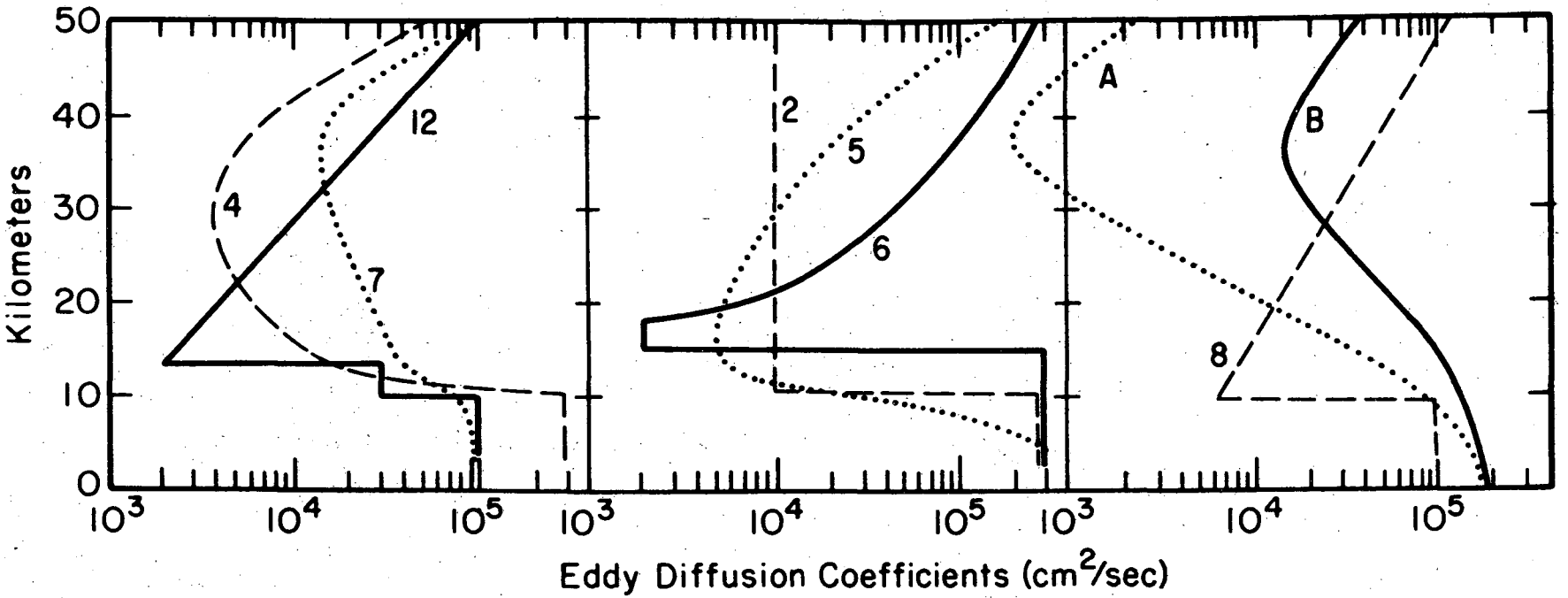
50
40
30
20
10
0
Kilometers
12
4
7
2
5
6
A
B
8
10^3
10^4
10^5
Eddy Diffusion Coefficients (cm^2/sec)
XBL751-5664

Fig. 2.

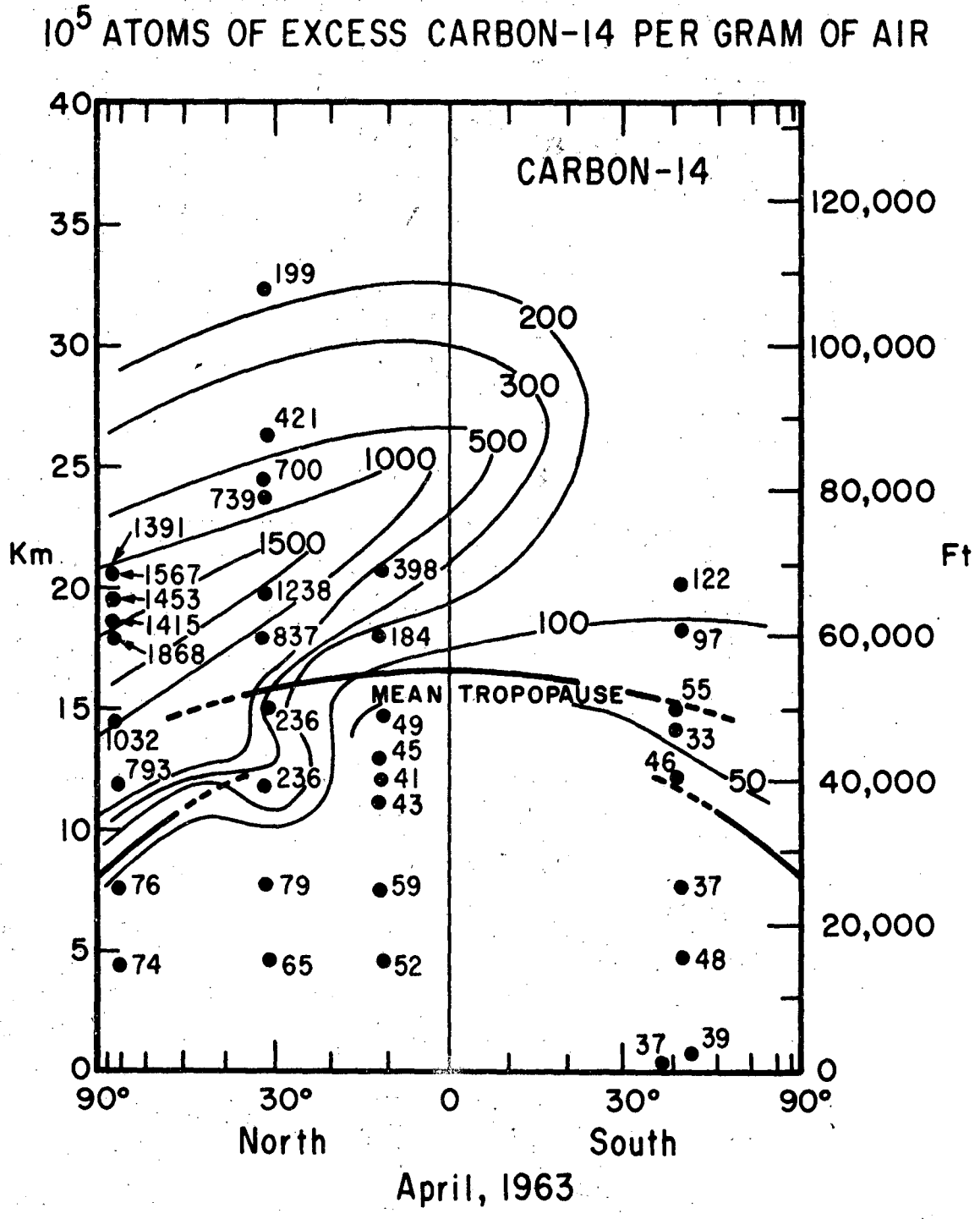

FIGURE 3

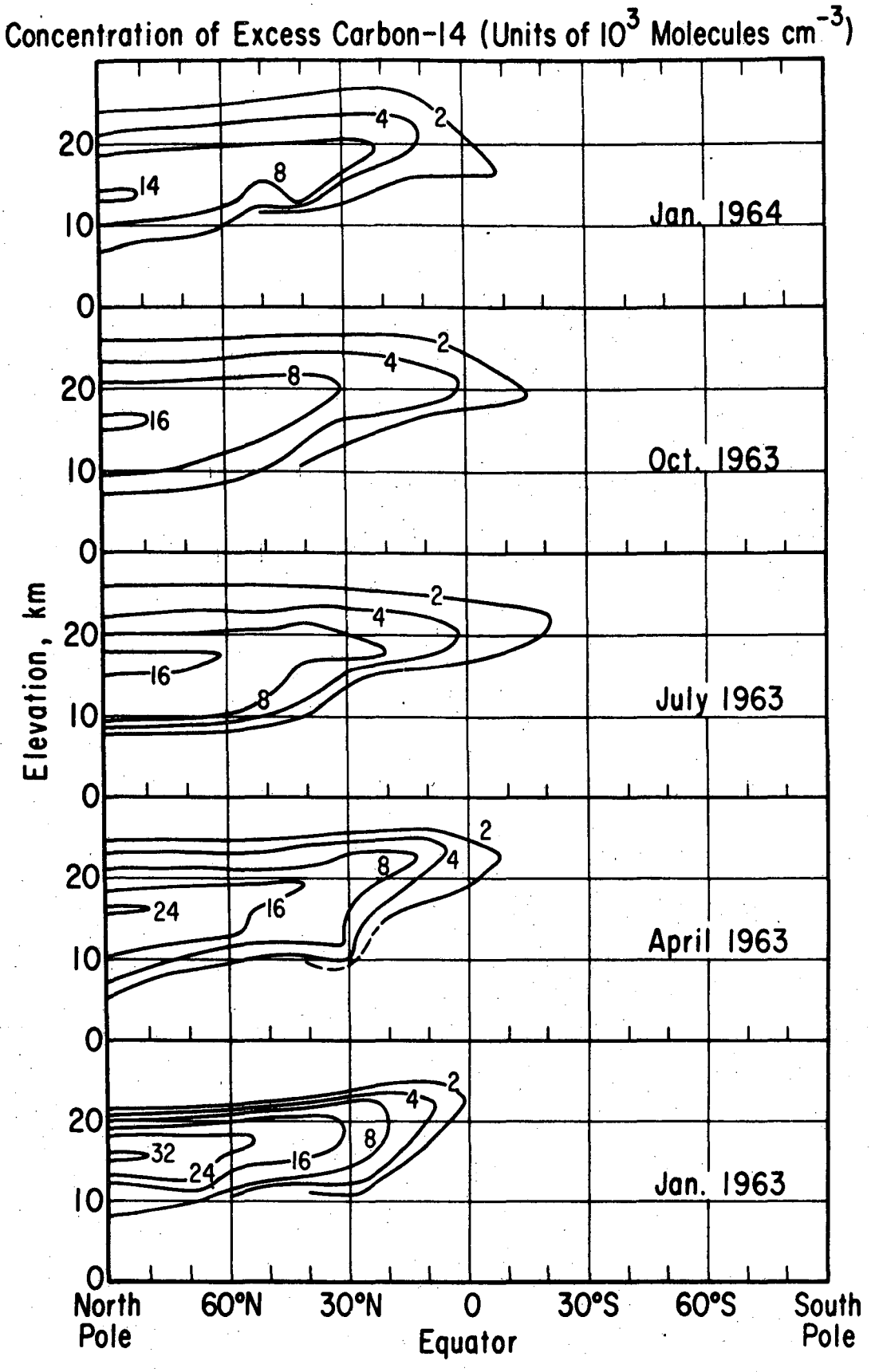
Concentration of Excess Carbon-14 (Units of 10^3 Molecules cm^{-3})
Elevation, km
Jan. 1964
Oct. 1963
July 1963
April 1963
Jan. 1963
North Pole
60°N
30°N
0
Equator
30°S
60°S
South Pole
XBL 741-5462

FIGURE 4

STRONTIUM-90
DISINTEGRATIONS PER MINUTE PER 1000 CUBIC FEET OF STANDARD AIR

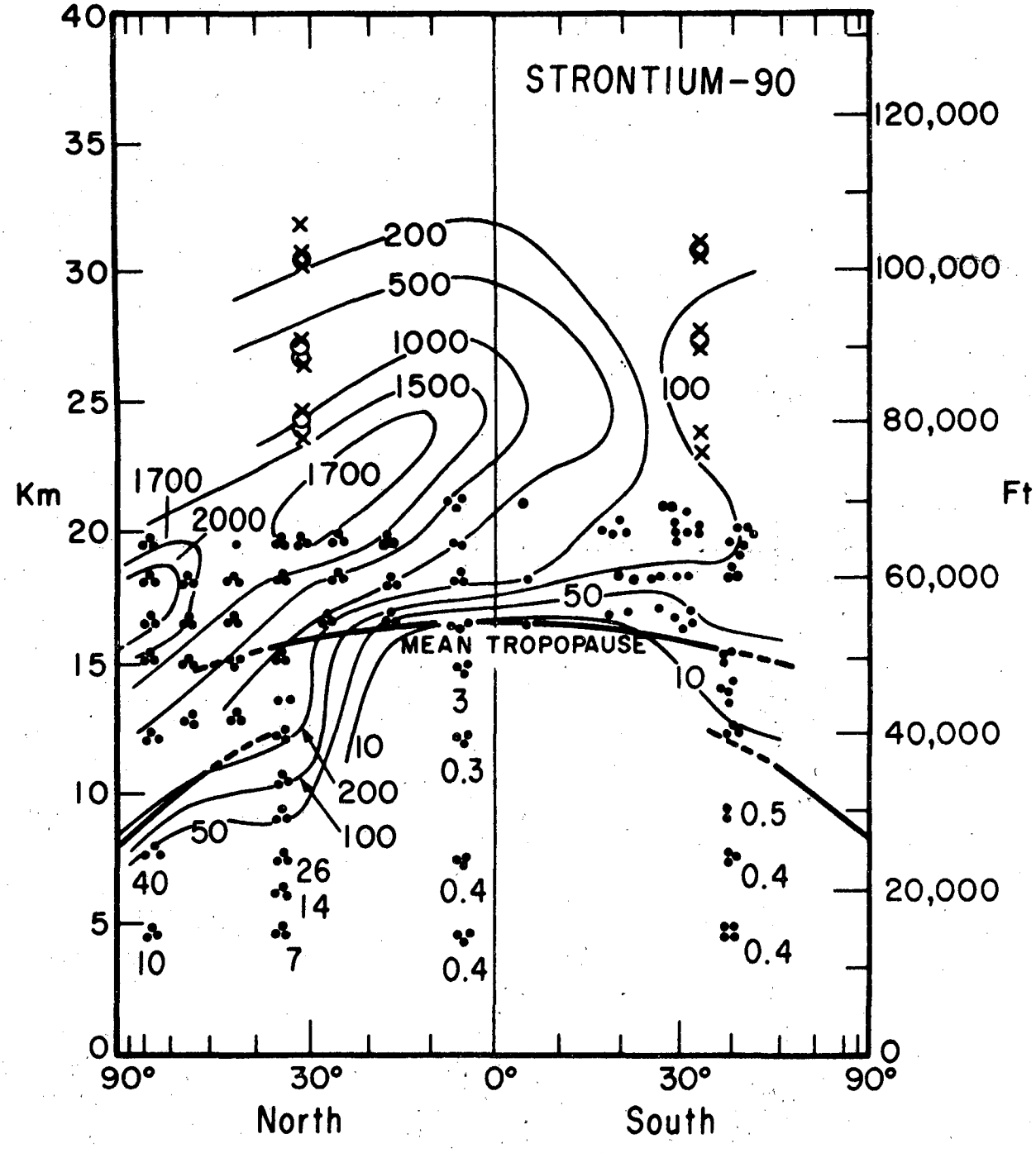

April, 1963

XBL 7410-7432

FIGURE 5

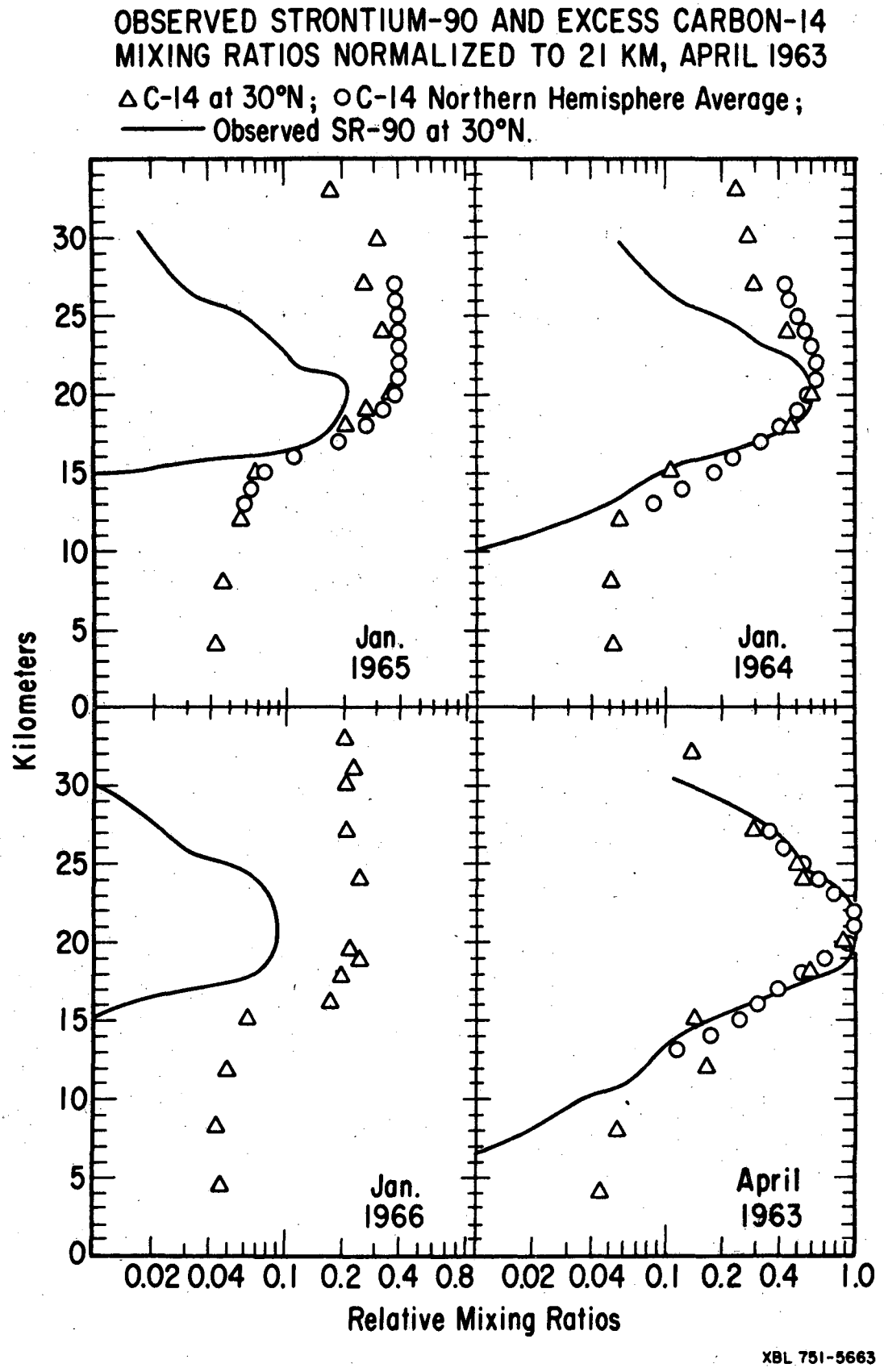
OBSERVED STRONTIUM-90 AND EXCESS CARBON-14
MIXING RATIOS NORMALIZED TO 21 KM, APRIL 1963
△ C-14 at 30°N; ○ C-14 Northern Hemisphere Average;
—— Observed SR-90 at 30°N.
Kilometers
30
25
20
15
10
5
0
Jan. 1965
Jan. 1964
Jan. 1966
April 1963
0.02 0.04 0.1 0.2 0.4 0.8
0.02 0.04 0.1 0.2 0.4 1.0
Relative Mixing Ratios
XBL 751-5663

Fig. 6.

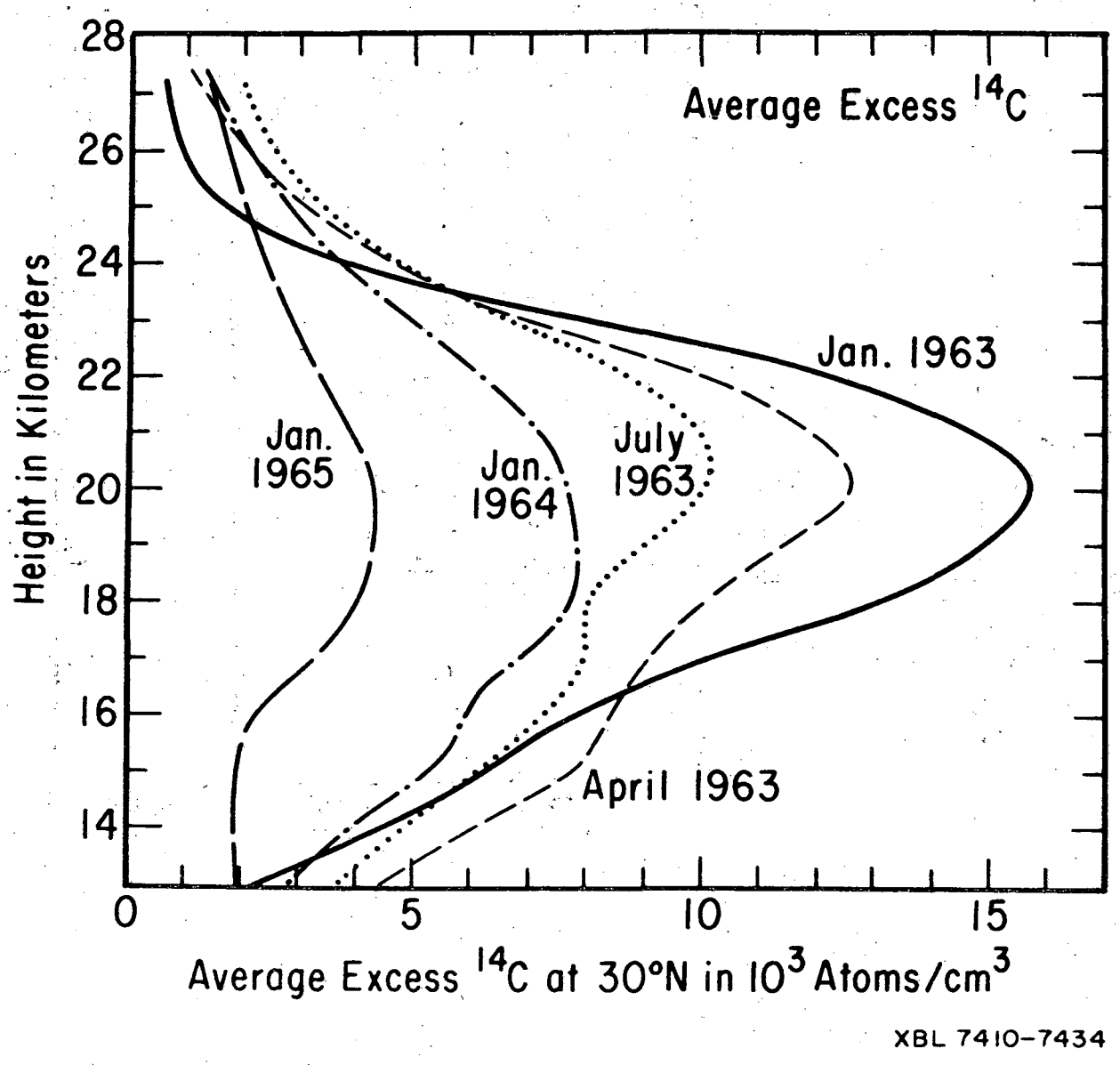

FIGURE 7

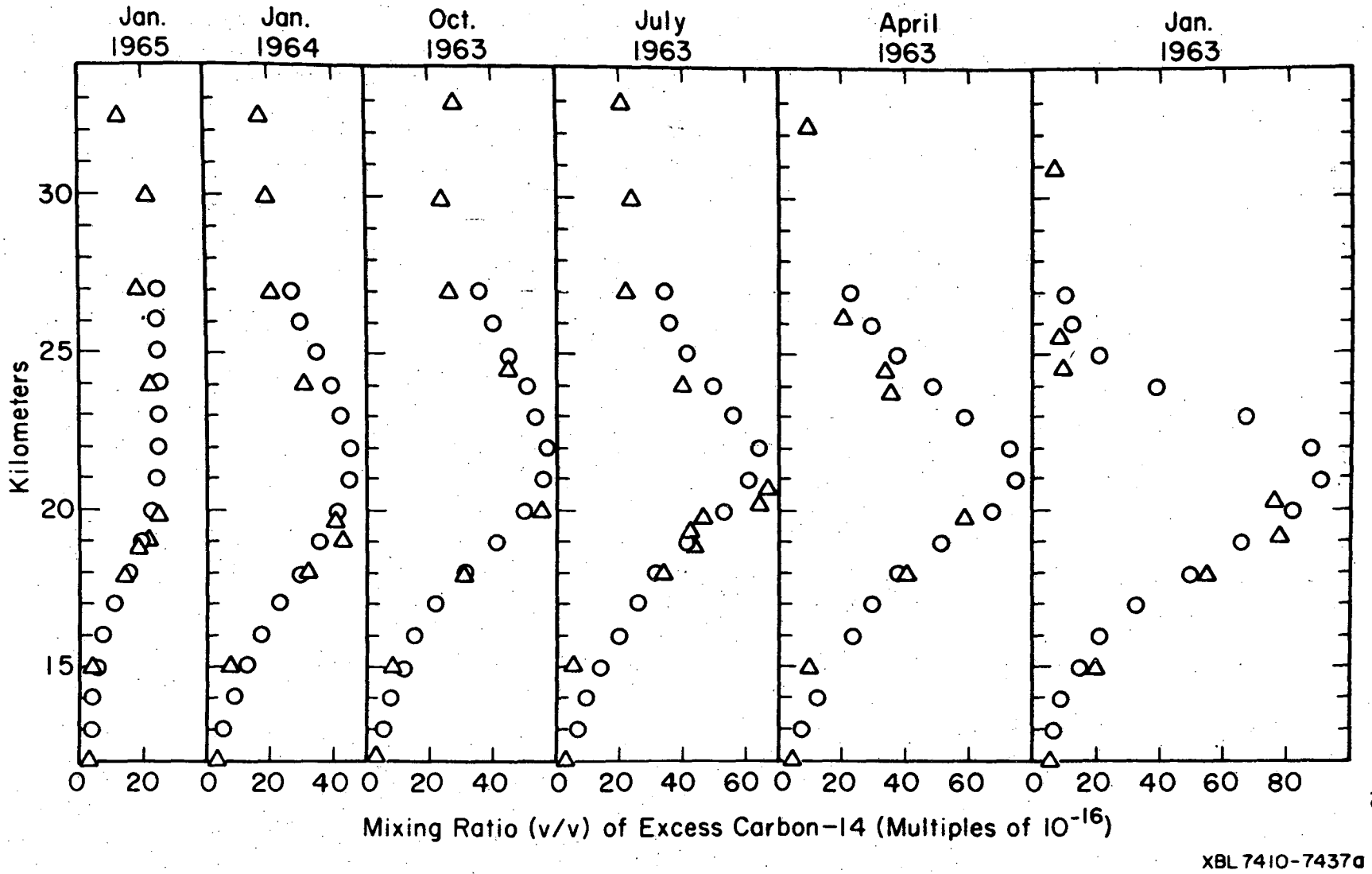
Jan. 1965
Jan. 1964
Oct. 1963
July 1963
April 1963
Jan. 1963
Kilometers
30
25
20
15
0 20
0 20 40
0 20 40
0 20 40 60
0 20 40 60
0 20 40 60 80
Mixing Ratio (v/v) of Excess Carbon-14 (Multiples of 10^{-16})
XBL 7410-7437a

FIGURE 8

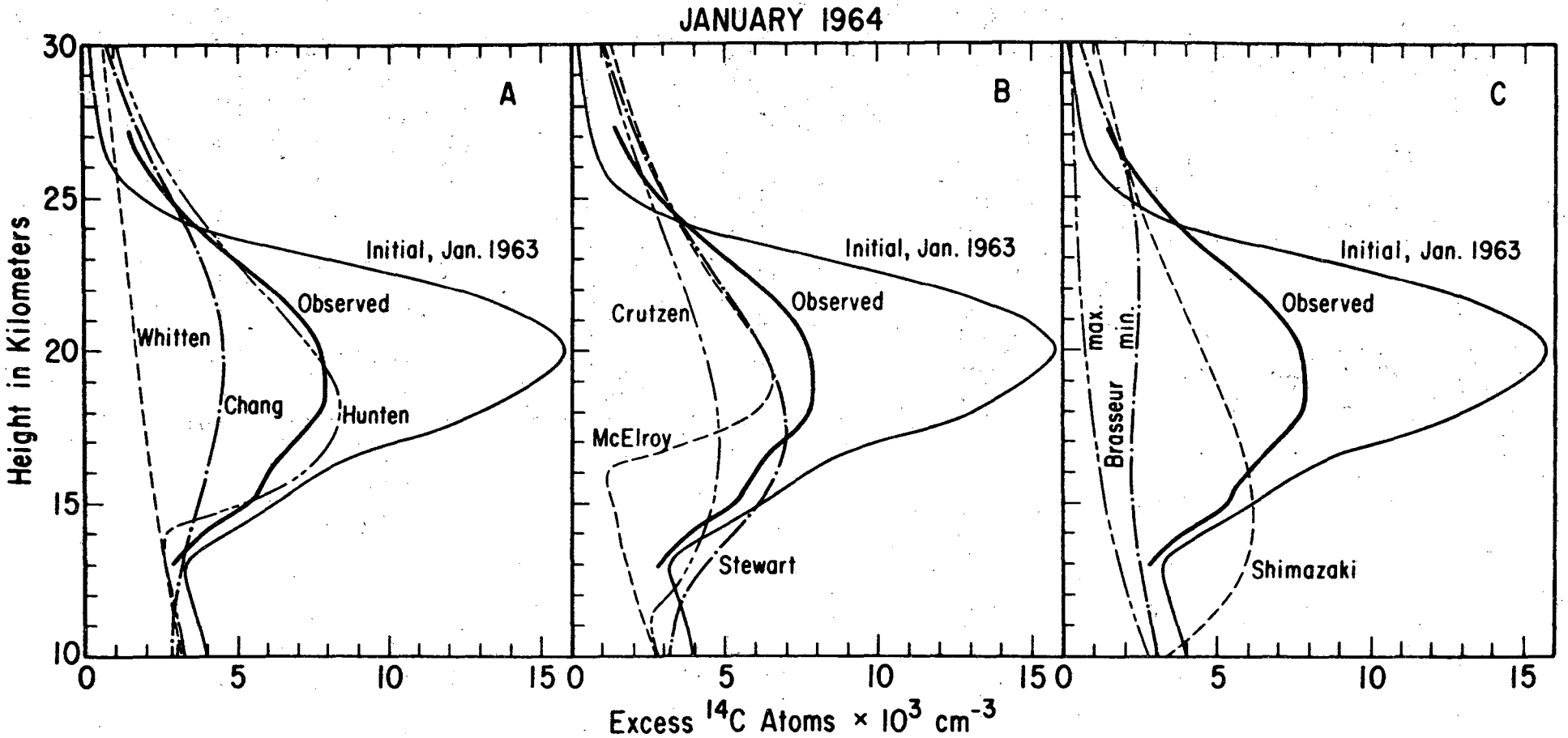

XBL 7410-7436

FIGURE 9

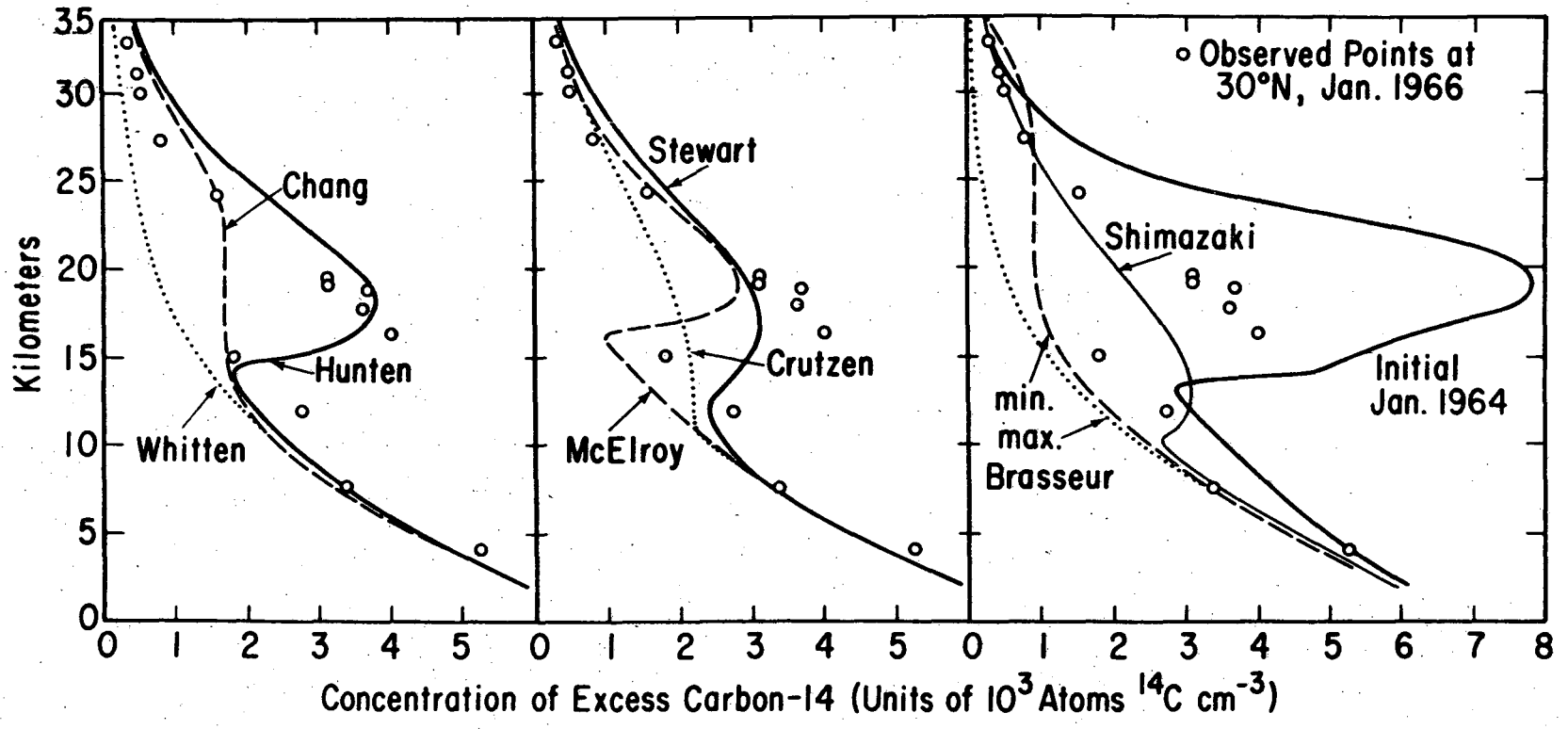

FIGURE 10

XBL-7412-7640

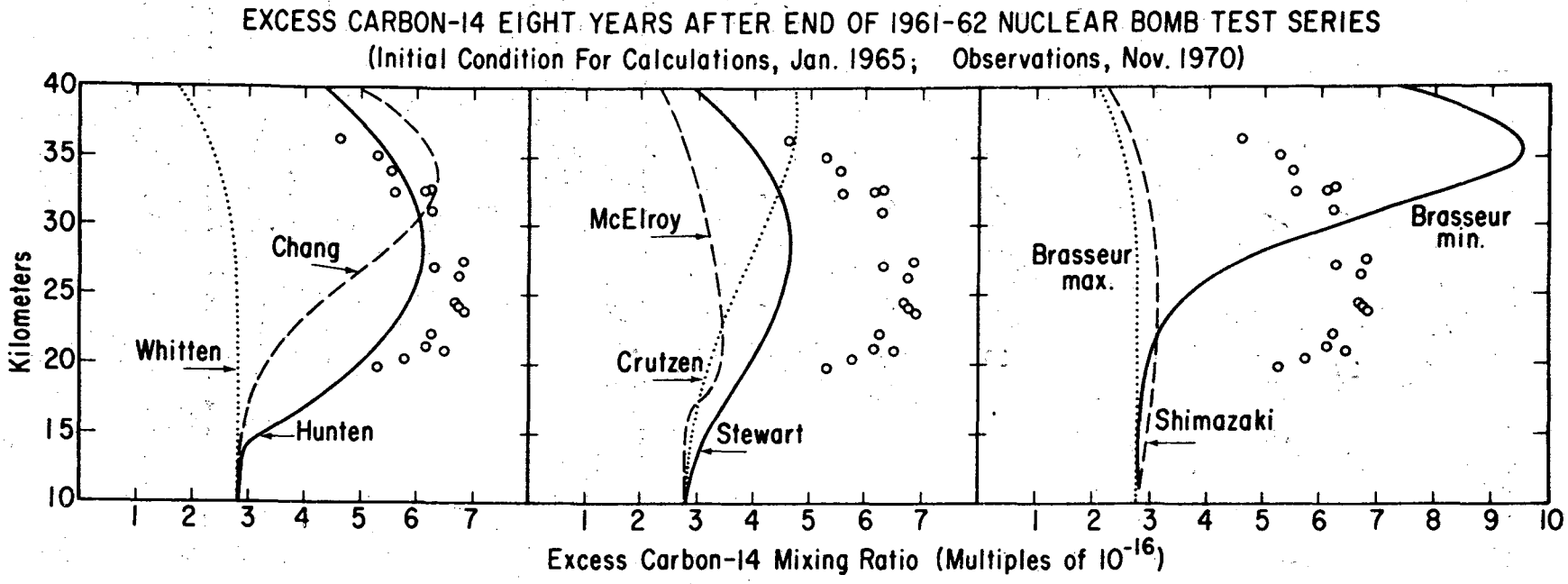

FIGURE 11

XBL-7412-7641

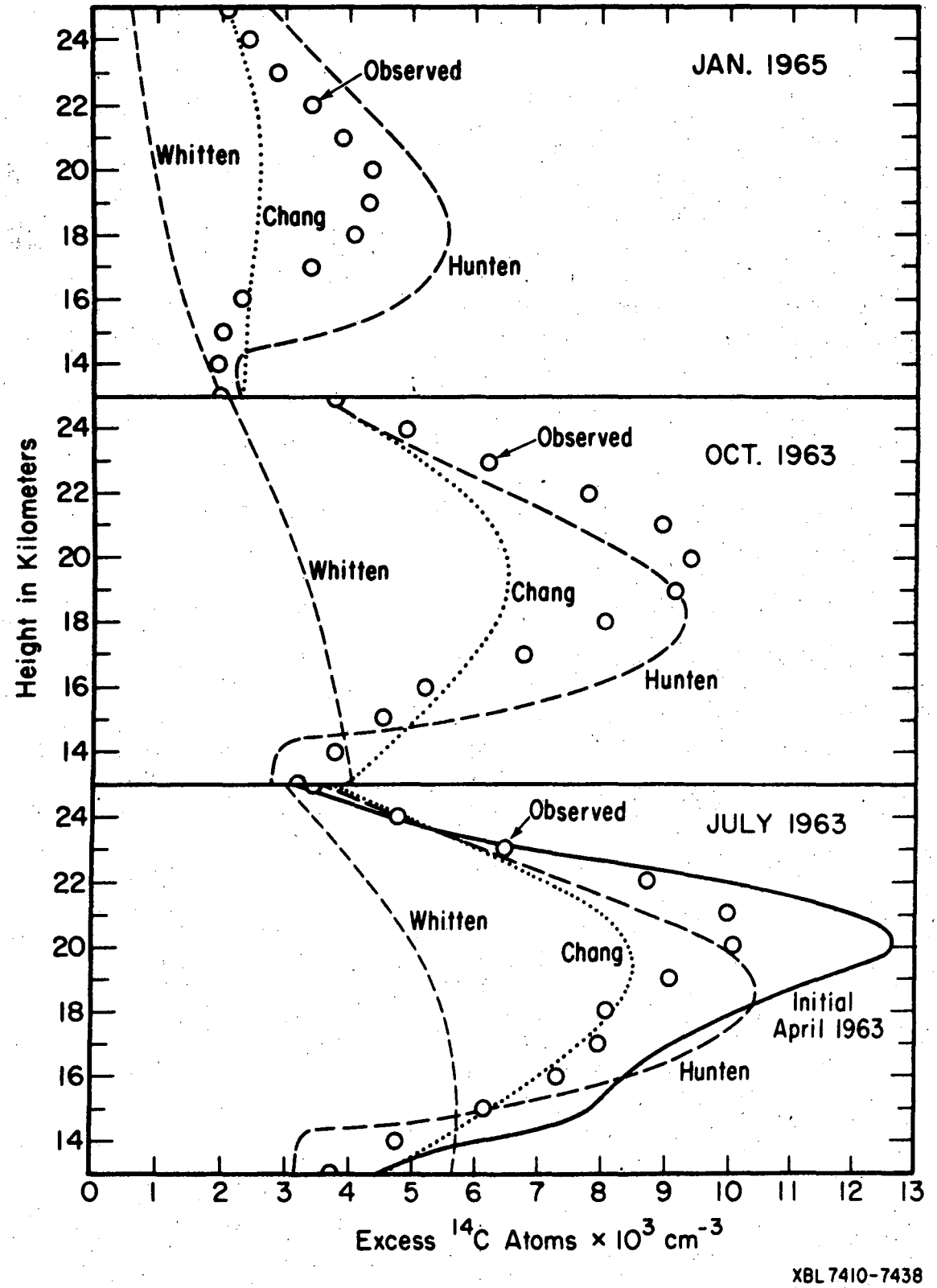
JAN. 1965
Observed
Whitten
Chang
Hunten
OCT. 1963
Observed
Whitten
Chang
Hunten
JULY 1963
Observed
Whitten
Chang
Initial
April 1963
Hunten
Height in Kilometers
Excess ^{14}C Atoms $\times 10^3$ cm^{-3}
XBL 7410-7438

Fig. 12.

Calculated and Observed Carbon-14 in the Stratosphere One, Two, Three, and Eight Years After January 1963. (Corrected for transport to southern hemisphere.) Calculated by Hunten's model; ○,● northern hemisphere average; △,▲ direct observations at 30°N.

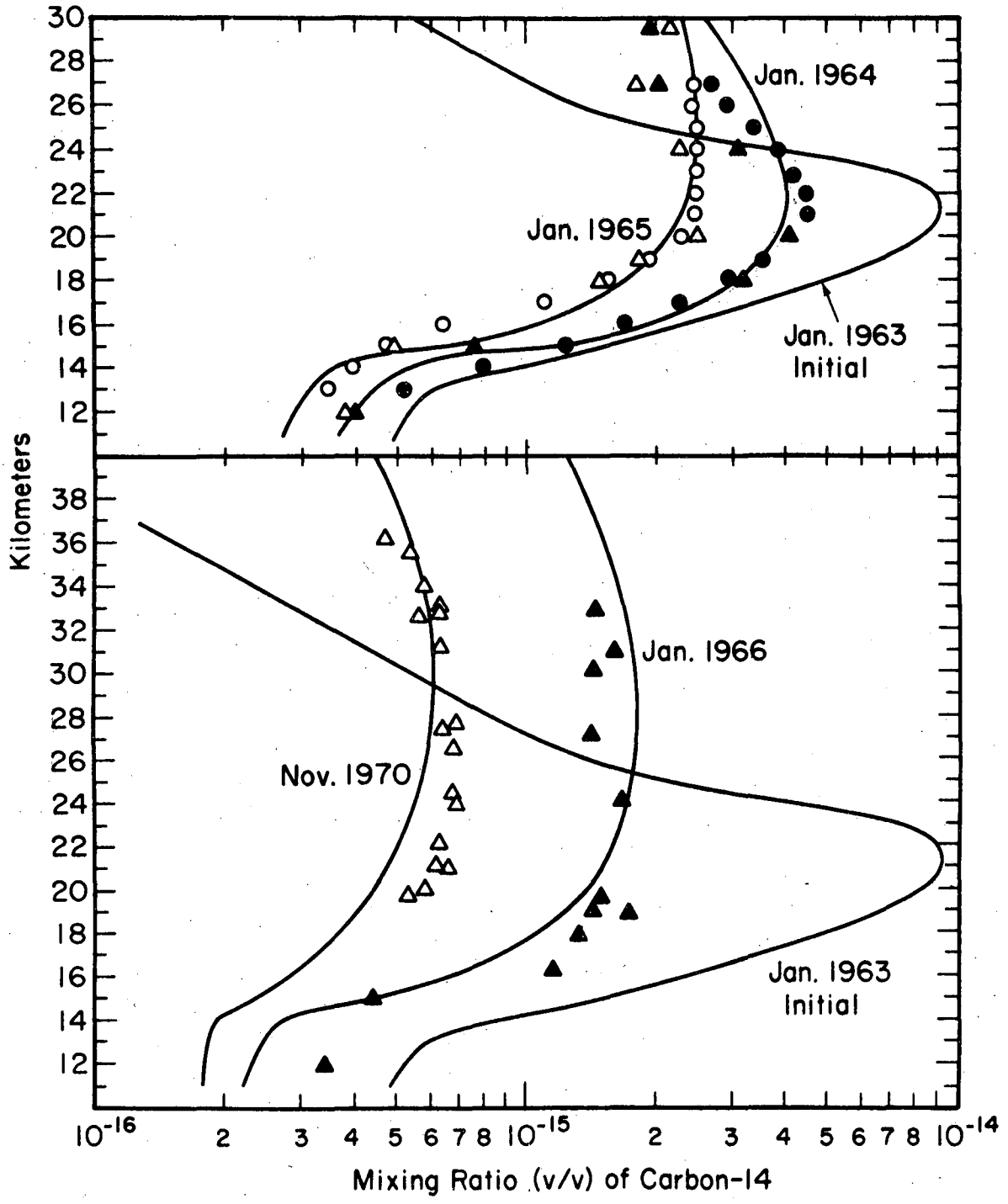

Fig. 13.

TECHNICAL INFORMATION DIVISION
LAWRENCE BERKELEY LABORATORY
UNIVERSITY OF CALIFORNIA
BERKELEY, CALIFORNIA 94720